

$$\overline{Nu}_\delta = 0.42 Ra_\delta^{0.25} Pr^{0.012} (\delta/H)^{0.3}$$

for  $10 < H/\delta < 40$ ,  $1 < Pr < 2 \times 10^4$ , and  $10^4 < Ra_\delta < 10^7$ .

### 43.3.4 The Log Mean Temperature Difference

The simplest and most common type of heat exchanger is the *double-pipe heat exchanger*, illustrated in Fig. 43.15. For this type of heat exchanger, the heat transfer between the two fluids can be found by assuming a constant overall heat transfer coefficient found from Table 43.8 and a constant fluid specific heat. For this type, the heat transfer is given by

$$q = UA \Delta T_m$$

where

$$\Delta T_m = \frac{\Delta T_2 - \Delta T_1}{\ln(\Delta T_2/\Delta T_1)}$$

In this expression, the temperature difference,  $\Delta T_m$ , is referred to as the *log-mean temperature difference* (LMTD);  $\Delta T_1$  represents the temperature difference between the two fluids at one end and  $\Delta T_2$  at the other end. For the case where the ratio  $\Delta T_2/\Delta T_1$  is less than two, the *arithmetic mean temperature difference*  $(\Delta T_2 + \Delta T_1)/2$  may be used to calculate the heat-transfer rate without introducing any significant error. As shown in Fig. 43.15,

$$\begin{aligned} \Delta T_1 &= T_{h,j} - T_{c,i} & \Delta T_2 &= T_{h,o} - T_{c,o} & \text{for parallel flow} \\ \Delta T_1 &= T_{h,i} - T_{c,o} & \Delta T_2 &= T_{h,o} - T_{c,i} & \text{for counterflow} \end{aligned}$$

### Cross-Flow Coefficient

In other types of heat exchangers, where the values of the overall heat transfer coefficient,  $U$ , may vary over the area of the surface, the LMTD may not be representative of the actual average temperature difference. In these cases, it is necessary to utilize a correction factor such that the heat transfer,  $q$ , can be determined by

$$q = UAF \Delta T_m$$

Here the value of  $\Delta T_m$  is computed assuming counterflow conditions,  $\Delta T_1 = T_{h,i} - T_{c,i}$  and  $\Delta T_2 = T_{h,o} - T_{c,o}$ . Figures 43.16 and 43.17 illustrate some examples of the *correction factor*,  $F$ , for various multiple-pass heat exchangers.

## 43.4 RADIATION HEAT TRANSFER

Heat transfer can occur in the absence of a participating medium through the transmission of energy by electromagnetic waves, characterized by a wavelength,  $\lambda$ , and frequency,  $\nu$ , which are related by  $c = \lambda\nu$ . The parameter  $c$  represents the velocity of light, which in a vacuum is  $c_o = 2.9979 \times 10^8$  m/sec. Energy transmitted in this fashion is referred to as *radiant energy* and the heat transfer process that occurs is called *radiation heat transfer* or simply *radiation*. In this mode of heat transfer, the energy is transferred through electromagnetic waves or through photons, with the energy of a photon being given by  $h\nu$ , where  $h$  represents Planck's constant.

In nature, every substance has a characteristic wave velocity that is smaller than that occurring in a vacuum. These velocities can be related to  $c_o$  by  $c = c_o/n$ , where  $n$  indicates the refractive index. The value of the refractive index  $n$  for air is approximately equal to 1. The wavelength of the energy given or for the radiation that comes from a surface depends on the nature of the source and various wavelengths sensed in different ways. For example, as shown in Fig. 43.18 the electromagnetic spectrum consists of a number of different types of radiation. Radiation in the visible spectrum occurs in the range  $\lambda = 0.4\text{--}0.74 \mu\text{m}$ , while radiation in the wavelength range  $0.1\text{--}100 \mu\text{m}$  is classified as *thermal radiation* and is sensed as heat. For radiant energy in this range, the amount of energy given off is governed by the temperature of the emitting body.

### 43.4.1 Black-Body Radiation

All objects in space are continuously being bombarded by radiant energy of one form or another and all of this energy is either absorbed, reflected, or transmitted. An ideal body that absorbs all the radiant energy falling upon it, regardless of the wavelength and direction, is referred to as a *black body*. Such a body emits the maximum energy for a prescribed temperature and wavelength. Radiation from a black body is independent of direction and is referred to as a *diffuse emitter*.

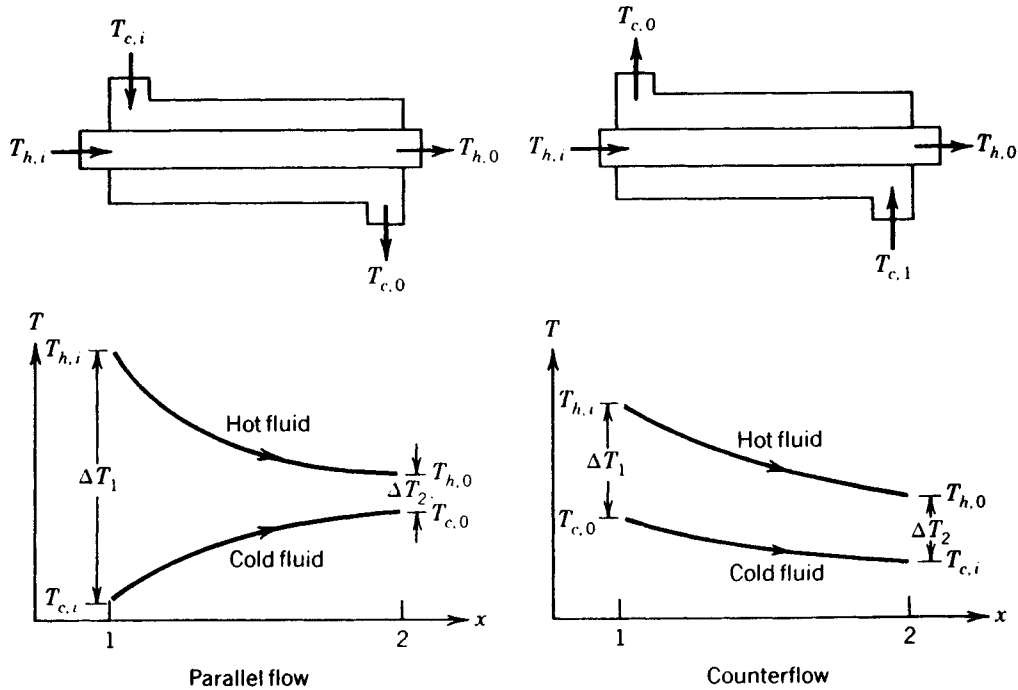


**Fig. 43.15** Temperature profiles for parallel flow and counterflow in double-pipe heat exchanger.

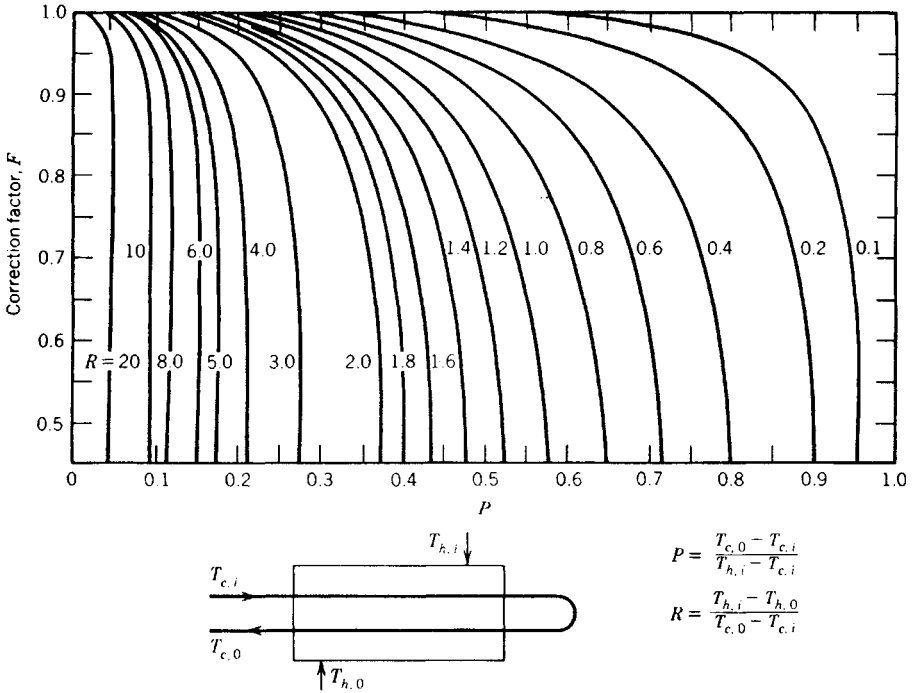


**Fig. 43.16** Correction factor for a shell-and-tube heat exchanger with one shell and any multiple of two tube passes (two, four, etc., tube passes).

**The Stefan-Boltzmann Law**

The Stefan-Boltzmann law describes the rate at which energy is radiated from a black body and states that this radiation is proportional to the fourth power of the absolute temperature of the body

$$e_b = \sigma T^4$$

where  $e_b$  is the total emissive power and  $\sigma$  is the Stefan-Boltzmann constant, which has the value  $5.729 \times 10^{-8} \text{ W/m}^2 \cdot \text{K}^4$  ( $0.173 \times 10^{-8} \text{ Btu/hr} \cdot \text{ft}^2 \cdot \text{R}^4$ ).

**Planck's Distribution Law**

The temperature dependent amount of energy leaving a black body is described as the spectral emissive power  $e_{bb}$  and is a function of wavelength. This function, which was derived from quantum theory by Planck, is

$$e_{\lambda b} = 2\pi C_1 / \lambda^5 [\exp(C_2 / \lambda T) - 1]$$

where  $e_{bb}$  has a unit  $\text{W/m}^2 \cdot \mu\text{m}$  ( $\text{Btu/hr} \cdot \text{ft}^2 \cdot \mu\text{m}$ ).

Values of the constants  $C_1$  and  $C_2$  are  $0.59544 \times 10^{-16} \text{ W} \cdot \text{m}^2$  ( $0.18892 \times 10^8 \text{ Btu} \cdot \mu\text{m}^4 / \text{hr ft}^2$ ) and  $14,388 \mu\text{m} \cdot \text{K}$  ( $25,898 \mu\text{m} \cdot \text{R}$ ), respectively. The distribution of the spectral emissive power from a black body at various temperatures is shown in Fig. 43.19, where, as shown, the energy emitted at all wavelengths increases as the temperature increases. The maximum or peak values of the constant temperature curves illustrated in Fig. 43.20 shift to the left for shorter wavelengths as the temperatures increase.

The fraction of the emissive power of a black body at a given temperature and in the wavelength interval between  $\lambda_1$  and  $\lambda_2$  can be described by

$$F_{\lambda_1 T - \lambda_2 T} = \frac{1}{\sigma T^4} \left( \int_{\lambda_1}^{\lambda_2} e_{\lambda b} d\lambda - \int_0^{\lambda_1} e_{\lambda b} d\lambda \right) = F_{\sigma - \lambda_1 T} - F_{\sigma - \lambda_2 T}$$

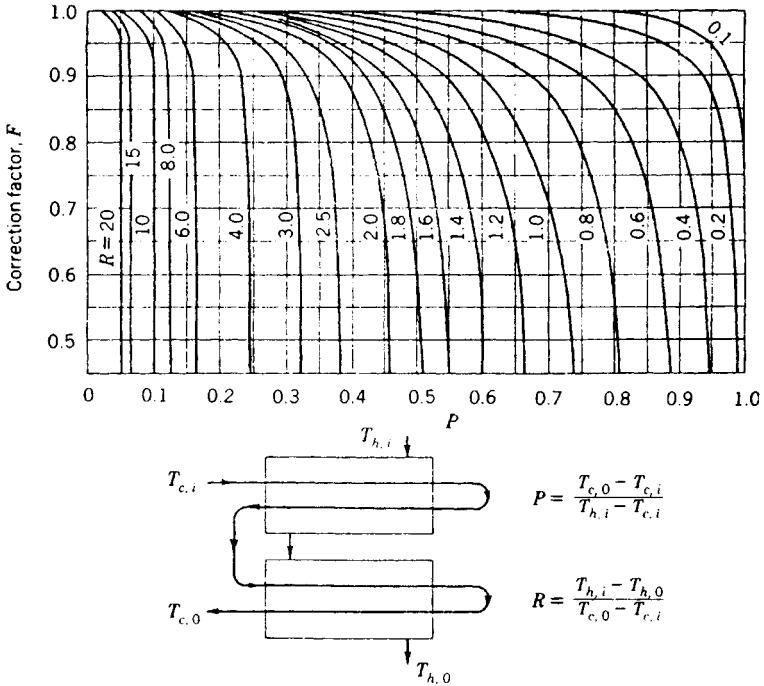


Fig. 43.17 Correction factor for a shell-and-tube heat exchanger with two shell passes and any multiple of four tubes passes (four, eight, etc., tube passes).

where the function  $F_{o-\lambda T} = (1/\sigma T^4) \int_0^\lambda e_{\lambda b} d\lambda$  is given in Table 43.16. This function is useful for the evaluation of total properties involving integration on the wavelength in which the spectral properties are piecewise constant.

**Wien's Displacement Law**

The relationship between these peak or maximum temperatures can be described by *Wien's displacement law*,

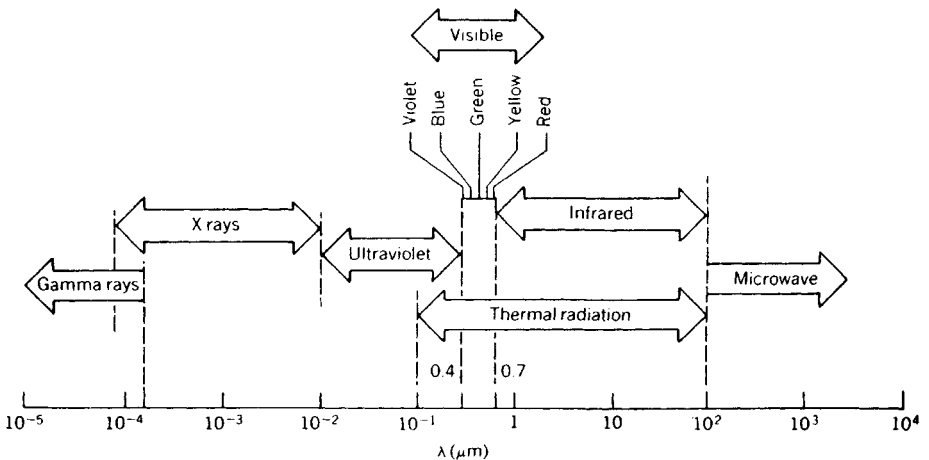


Fig. 43.18 Electromagnetic radiation spectrum.

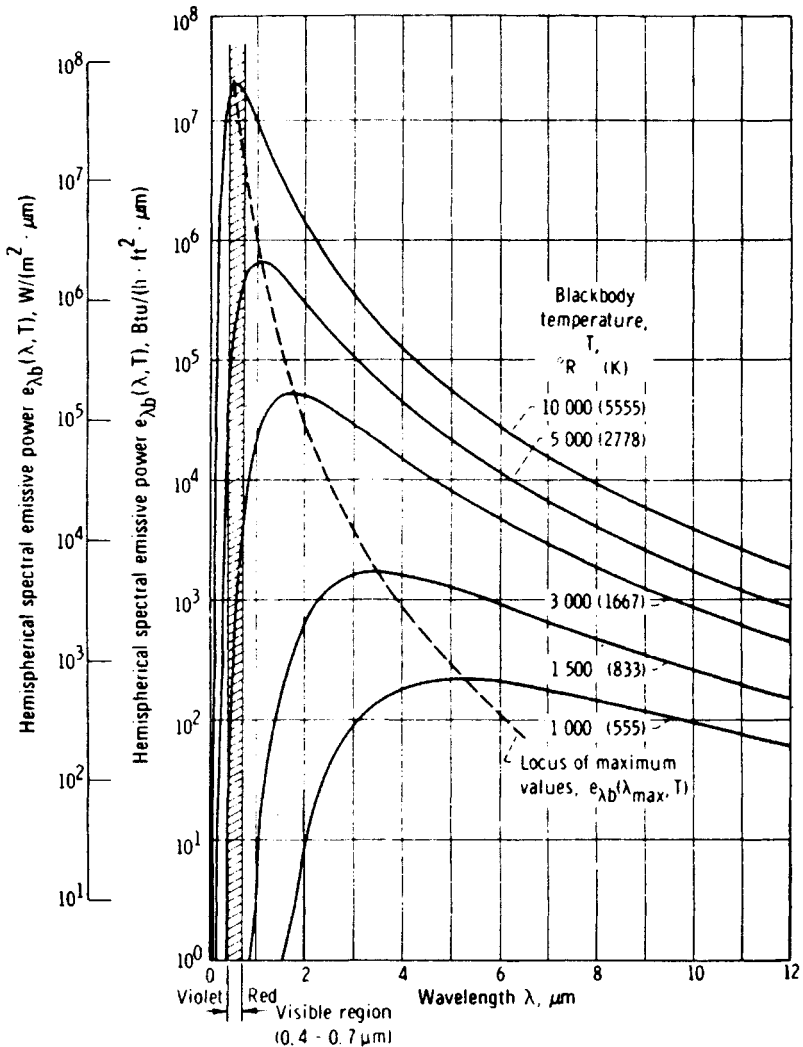


Fig. 43.19 Hemispherical spectral emissive power of a black-body for various temperatures.

$$\lambda_{\max} T = 2897.8 \mu\text{m} \cdot \text{K}$$

or

$$\lambda_{\max} T = 5216.0 \mu\text{m} \cdot ^\circ\text{R}$$

#### 43.4.2 Radiation Properties

While, to some degree, all surfaces follow the general trends described by the Stefan-Boltzmann and Planck laws, the behavior of real surfaces deviates somewhat from these. In fact, because black bodies are ideal, all real surfaces emit and absorb less radiant energy than a black body. The amount of energy a body emits can be described in terms of the emissivity and is, in general, a function of the type of material, the temperature, and the surface conditions, such as roughness, oxide layer thickness, and chemical contamination. The emissivity is in fact a measure of how well a real body radiates energy as compared with a black body of the same temperature. The radiant energy emitted into the entire hemispherical space above a real surface element, including all wavelengths, is given

$$dA_i dF_{di-dj} = dA_j dF_{dj-di}$$

$$dA_i F_{di-j} = A_j dF_{j-di}$$

$$A_i F_{i-j} = A_j F_{j-i}$$

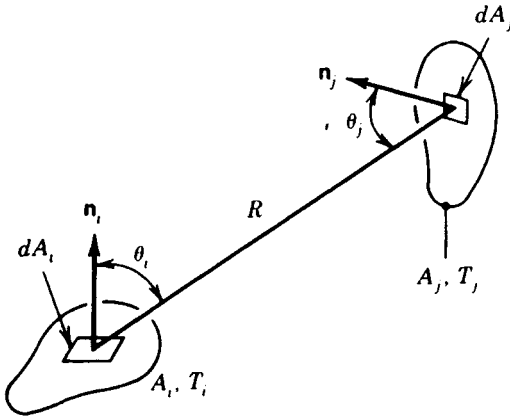


Fig. 43.20 Configuration factor for radiation exchange between surfaces of area  $dA_i$  and  $dA_j$ .

by  $e = \epsilon\sigma T^4$ , where  $\epsilon$  is less than 1.0, and is called the *hemispherical emissivity* (or *total hemispherical emissivity* to indicate integration over the total wavelength spectrum). For a given wavelength, the *spectral hemispherical emissivity*  $\epsilon_\lambda$  of a real surface is defined as

$$\epsilon_\lambda = e_\lambda / e_{\lambda b}$$

where  $e_\lambda$  is the hemispherical emissive power of the real surface and  $e_{\lambda b}$  is that of a black body at the same temperature.

*Spectral irradiation*  $G_\lambda$  ( $\text{W}/\text{m}^2 \cdot \mu\text{m}$ ) is defined as the rate at which radiation is incident upon a surface per unit area of the surface, per unit wavelength about the wavelength  $\lambda$ , and encompasses the incident radiation from all directions.

*Spectral hemispherical reflectivity*  $\rho_\lambda$  is defined as the radiant energy reflected per unit time, per unit area of the surface, per unit wavelength/ $G_\lambda$ .

*Spectral hemispherical absorptivity*  $\alpha_\lambda$ , is defined as the radiant energy absorbed per unit area of the surface, per unit wavelength about the wavelength/ $G_\lambda$ .

*Spectral hemispherical transmissivity* is defined as the radiant energy transmitted per unit area of the surface, per unit wavelength about the wavelength/ $G_\lambda$ .

For any surface, the sum of the reflectivity, absorptivity and transmissivity must equal unity, that is,

$$\alpha_\lambda + \rho_\lambda + \tau_\lambda = 1$$

When these values are integrated over the entire wavelength from  $\lambda = 0$  to  $\infty$  they are referred to as *total values*. Hence, the *total hemispherical reflectivity*, *total hemispherical absorptivity*, and *total hemispherical transmissivity* can be written as

$$\rho = \int_0^\infty \rho_\lambda G_\lambda d\lambda / G$$

$$\alpha = \int_0^\infty \alpha_\lambda G_\lambda d\lambda / G$$

and

**Table 43.16** Radiation Function  $F_{0-\lambda T}$ 

$\lambda T$		$F_{0-\lambda T}$	$\lambda T$		$F_{0-\lambda T}$	$\lambda T$		$F_{0-\lambda T}$
$\mu\text{m} \cdot \text{K}$	$\mu\text{m} \cdot ^\circ\text{R}$		$\mu\text{m} \cdot \text{K}$	$\mu\text{m} \cdot ^\circ\text{R}$		$\mu\text{m} \cdot \text{K}$	$\mu\text{m} \cdot ^\circ\text{R}$	
400	720	$0.1864 \times 10^{-11}$	3400	6120	0.3617	6400	11,520	0.7692
500	900	$0.1298 \times 10^{-8}$	3500	6300	0.3829	6500	11,700	0.7763
600	1080	$0.9290 \times 10^{-7}$	3600	6480	0.4036	6600	11,880	0.7832
700	1260	$0.1838 \times 10^{-5}$	3700	6660	0.4238	6800	12,240	0.7961
800	1440	$0.1643 \times 10^{-4}$	3800	6840	0.4434	7000	12,600	0.8081
900	1620	$0.8701 \times 10^{-4}$	3900	7020	0.4624	7200	12,960	0.8192
1000	1800	$0.3207 \times 10^{-3}$	4000	7200	0.4809	7400	13,320	0.8295
1100	1980	$0.9111 \times 10^{-3}$	4100	7380	0.4987	7600	13,680	0.8391
1200	2160	$0.2134 \times 10^{-2}$	4200	7560	0.5160	7800	14,040	0.8480
1300	2340	$0.4316 \times 10^{-2}$	4300	7740	0.5327	8000	14,400	0.8562
1400	2520	$0.7789 \times 10^{-2}$	4400	7920	0.5488	8200	14,760	0.8640
1500	2700	$0.1285 \times 10^{-1}$	4500	8100	0.5643	8400	15,120	0.8712
1600	2880	$0.1972 \times 10^{-1}$	4600	8280	0.5793	8600	15,480	0.8779
1700	3060	$0.2853 \times 10^{-1}$	4700	8460	0.5937	8800	15,840	0.8841
1800	3240	$0.3934 \times 10^{-1}$	4800	8640	0.6075	9000	16,200	0.8900
1900	3420	$0.5210 \times 10^{-1}$	4900	8820	0.6209	10,000	18,000	0.9142
2000	3600	$0.6673 \times 10^{-1}$	5000	9000	0.6337	11,000	19,800	0.9318
2100	3780	$0.8305 \times 10^{-1}$	5100	9180	0.6461	12,000	21,600	0.9451
2200	3960	0.1009	5200	9360	0.6579	13,000	23,400	0.9551
2300	4140	0.1200	5300	9540	0.6694	14,000	25,200	0.9628
2400	4320	0.1402	5400	9720	0.6803	15,000	27,000	0.9689
2500	4500	0.1613	5500	9900	0.6909	20,000	36,000	0.9856
2600	4680	0.1831	5600	10,080	0.7010	25,000	45,000	0.9922
2700	4860	0.2053	5700	10,260	0.7108	30,000	54,000	0.9953
2800	5040	0.2279	5800	10,440	0.7201	35,000	63,000	0.9970
2900	5220	0.2505	5900	10,620	0.7291	40,000	72,000	0.9979
3000	5400	0.2732	6000	10,800	0.7378	45,000	81,000	0.9985
3100	5580	0.2058	6100	10,980	0.7461	50,000	90,000	0.9989
3200	5760	0.3181	6200	11,160	0.7541	55,000	99,000	0.9992
3300	5940	0.3401	6300	11,340	0.7618	60,000	108,000	0.9994

$$\tau = \int_0^{\infty} \tau_{\lambda} G_{\lambda} d\lambda / G$$

respectively, where

$$G = \int_0^{\infty} G_{\lambda} d\lambda$$

As was the case for the wavelength-dependent parameters, the sum of the total reflectivity, total absorptivity, and total transmissivity must be equal to unity, that is,

$$\alpha + \rho + \tau = 1$$

It is important to note that while the emissivity is a function of the material, temperature, and surface conditions, the absorptivity and reflectivity depend on both the surface characteristics and the nature of the incident radiation.

The terms *reflectance*, *absorptance*, and *transmittance* are used by some authors for the real surfaces and the terms *reflectivity*, *absorptivity*, and *transmissivity* are reserved for the properties of the ideal surfaces (i.e., those optically smooth and pure substances perfectly uncontaminated). Sur-

faces that allow no radiation to pass through are referred to as *opaque*, that is,  $\tau_\lambda = 0$ , and all of the incident energy will be either reflected or absorbed. For such a surface,

$$\alpha_\lambda + \rho_\lambda = 1$$

and

$$\alpha + \rho = 1$$

Light rays reflected from a surface can be reflected in such a manner that the incident and reflected rays are symmetric with respect to the surface normal at the point of incidence. This type of radiation is referred to as *specular*. The radiation is referred to as *diffuse* if the intensity of the reflected radiation is uniform over all angles of reflection and is independent of the incident direction, and the surface is called a *diffuse surface* if the radiation properties are independent of the direction. If they are independent of the wavelength, the surface is called a *gray surface*, and a *diffuse-gray surface* absorbs a fixed fraction of incident radiation from any direction and at any wavelength, and  $\alpha_\lambda = \epsilon_\lambda = \alpha = \epsilon$ .

### Kirchhoff's Law of Radiation

The directional characteristics can be specified by the addition of a ' to the value. For example the spectral emissivity for radiation in a particular direction would be denoted by  $\alpha'_\lambda$ . For radiation in a particular direction, the spectral emissivity is equal to the directional spectral absorptivity for the surface irradiated by a black body at the same temperature. The most general form of this expression states that  $\alpha'_\lambda = \epsilon'_\lambda$ . If the incident radiation is independent of angle or if the surface is diffuse, then  $\alpha_\lambda = \epsilon_\lambda$  for the hemispherical properties. This relationship can have various conditions imposed, depending on whether the spectral, total, directional, or hemispherical quantities are being considered.<sup>19</sup>

### Emissivity of Metallic Surfaces

The properties of pure smooth metallic surfaces are often characterized by low emissivity and absorptivity values and high values of reflectivity. The spectral emissivity of metals tends to increase with decreasing wavelength and exhibits a peak near the visible region. At wavelengths  $\lambda > \sim 5 \mu\text{m}$ , the spectral emissivity increases with increasing temperature; however, this trend reverses at shorter wavelengths ( $\lambda < \sim 1.27 \mu\text{m}$ ). Surface roughness has a pronounced effect on both the hemispherical emissivity and absorptivity, and large *optical roughnesses*, defined as the mean square roughness of the surface divided by the wavelength, will increase the hemispherical emissivity. For cases where the optical roughness is small, the directional properties will approach the values obtained for smooth surfaces. The presence of impurities, such as oxides or other nonmetallic contaminants, will change the properties significantly and increase the emissivity of an otherwise pure metallic body. A summary of the normal total emissivities for metals is given in Table 43.17. It should be noted that the hemispherical emissivity for metals is typically 10–30% higher than the values typically encountered for normal emissivity.

### Emissivity of Nonmetallic Materials

Large values of total hemispherical emissivity and absorptivity are typical for nonmetallic surfaces at moderate temperatures and, as shown in Table 43.18, which lists the normal total emissivity of some nonmetals, the temperature dependence is small.

### Absorptivity for Solar Incident Radiation

The spectral distribution of solar radiation can be approximated by black-body radiation at a temperature of approximately 5800 K (10,000°R) and yields an average solar irradiation at the outer limit of the atmosphere of approximately 1353 W/m<sup>2</sup> (429 Btu/ft<sup>2</sup>·hr). This solar irradiation is called the *solar constant* and is greater than the solar irradiation received at the surface of the earth, due to the radiation scattering by air molecules, water vapor, and dust, and the absorption by O<sub>3</sub>, H<sub>2</sub>O, and CO<sub>2</sub> in the atmosphere. The absorptivity of a substance depends not only on the surface properties but also on the sources of incident radiation. Since solar radiation is concentrated at a shorter wavelength, due to the high source temperature, the absorptivity for certain materials when exposed to solar radiation may be quite different from that for low-temperature radiation, where the radiation is concentrated in the longer-wavelength range. A comparison of absorptivities for a number of different materials is given in Table 43.19 for both solar and low-temperature radiation.

#### 43.4.3 Configuration Factor

The magnitude of the radiant energy exchanged between any two given surfaces is a function of the emissivity, absorptivity, and transmissivity. In addition, the energy exchange is a strong function of



**Table 43.17 Normal Total Emissivity of Metals<sup>a</sup>**

Materials	Surface Temperature (K)	Normal Total Emissivity
Aluminum		
Highly polished plate	480–870	0.038–0.06
Polished plate	373	0.095
Heavily oxidized	370–810	0.20–0.33
Bismuth, bright	350	0.34
Chromium, polished	310–1370	0.08–0.40
Copper		
Highly polished	310	0.02
Slightly polished	310	0.15
Black oxidized	310	0.78
Gold, highly polished	370–870	0.018–0.035
Iron		
Highly polished, electrolytic	310–530	0.05–0.07
Polished	700–760	0.14–0.38
Wrought iron, polished	310–530	0.28
Cast iron, rough, strongly oxidized	310–530	0.95
Lead		
Polished	310–530	0.06–0.08
Rough unoxidized	310	0.43
Mercury, unoxidized	280–370	0.09–0.12
Molybdenum, polished	310–3030	0.05–0.29
Nickel		
Electrolytic	310–530	0.04–0.06
Electroplated on iron, not polished	293	0.11
Nickel oxide	920–1530	0.59–0.86
Platinum, electrolytic	530–810	0.06–0.10
Silver, polished	310–810	0.01–0.03
Steel		
Polished sheet	90–420	0.07–0.14
Mild steel, polished	530–920	0.27–0.31
Sheet with rough oxide layer	295	0.81
Tin, polished sheet	310	0.05
Tungsten, clean	310–810	0.03–0.08
Zinc		
Polished	310–810	0.02–0.05
Gray oxidized	295	0.23–0.28

<sup>a</sup>Adapted from Ref. 19.

how one surface is viewed from the other. This aspect can be defined in terms of the *configuration factor* (sometimes called the *radiation shape factor*, *view factor*, *angle factor*, or *interception factor*). As shown in Fig. 43.20, the configuration factor  $F_{i-j}$  is defined as that fraction of the radiation leaving a black surface  $i$  that is intercepted by a black or gray surface  $j$ , and is based upon the relative geometry, position, and shape of the two surfaces. The configuration factor can also be expressed in terms of the differential fraction of the energy or  $dF_{i-dj}$ , which indicates the differential fraction of energy from a finite area  $A_i$  that is intercepted by an infinitesimal area  $dA_j$ . Expressions for a number of different cases are given below for several common geometries.

Infinitesimal area  $dA_i$  to infinitesimal area  $dA_j$

$$dF_{di-dj} = \frac{\cos\theta_i \cos\theta_j}{\pi R^2} dA_j$$

Infinitesimal area  $dA_i$  to finite area  $A_j$

**Table 43.18 Normal Total Emissivity of Nonmetals<sup>a</sup>**

Materials	Surface Temperature (K)	Normal Total Emissivity
Asbestos, board	310	0.96
Brick		
White refractory	1370	0.29
Rough red	310	0.93
Carbon, lampsoot	310	0.95
Concrete, rough	310	0.94
Ice, smooth	273	0.966
Magnesium oxide, refractory	420–760	0.69–0.55
Paint		
Oil, all colors	373	0.92–0.96
Lacquer, flat black	310–370	0.96–0.98
Paper, white	310	0.95
Plaster	310	0.91
Porcelain, glazed	295	0.92
Rubber, hard	293	0.92
Sandstone	310–530	0.83–0.90
Silicon carbide	420–920	0.83–0.96
Snow	270	0.82
Water, deep	273–373	0.96
Wood, sawdust	310	0.75

<sup>a</sup>Adapted from Ref. 19.**Table 43.19 Comparison of Absorptivities of Various Surfaces to Solar and Low-Temperature Thermal Radiation<sup>a</sup>**

Surface	Absorptivity	
	For Solar Radiation	For Low-Temperature Radiation (~300 K)
Aluminum, highly polished	0.15	0.04
Copper, highly polished	0.18	0.03
Tarnished	0.65	0.75
Cast iron	0.94	0.21
Stainless steel, No. 301, polished	0.37	0.60
White marble	0.46	0.95
Asphalt	0.90	0.90
Brick, red	0.75	0.93
Gravel	0.29	0.85
Flat black lacquer	0.96	0.95
White paints, various types of pigments	0.12–0.16	0.90–0.95

<sup>a</sup>Adapted from Ref. 20 after J. P. Holman, *Heat Transfer*, McGraw-Hill, New York, 1981.

$$F_{di-j} = \int_{A_j} \frac{\cos\theta_i \cos\theta_j}{\pi R^2} dA_j$$

Finite area  $A_i$  to finite area  $A_j$

$$F_{i-j} = \frac{1}{A_i} \int_{A_i} \int_{A_j} \frac{\cos\theta_i \cos\theta_j}{\pi R^2} dA_i dA_j$$

Analytical expressions of other configuration factors have been found for a wide variety of simple geometries. A number of these are presented in Figs. 43.21–43.24 for surfaces that emit and reflect diffusely.

### Reciprocity Relations

The configuration factors can be combined and manipulated using algebraic rules referred to as *configuration factor geometry*. These expressions take several forms, one of which is the reciprocal properties between different configuration factors that allow one configuration factor to be determined from knowledge of the others:

$$\begin{aligned} dA_i dF_{di-dj} &= dA_j dF_{dj-di} \\ dA_i dF_{di-j} &= A_j dF_{j-di} \\ A_i F_{i-j} &= A_j F_{j-i} \end{aligned}$$

These relationships can be combined with other basic rules to allow the determination of the configuration of an infinite number of complex shapes and geometries from a few select, known geometries. These are summarized in the following sections.

### The Additive Property

For a surface  $A_i$  subdivided into  $N$  parts ( $A_{i1}, A_{i2}, \dots, A_{iN}$ ) and a surface  $A_j$  subdivided into  $M$  parts ( $A_{j1}, A_{j2}, \dots, A_{jM}$ ),

$$A_i F_{i-j} = \sum_{n=1}^N \sum_{m=1}^M A_{in} F_{in-jm}$$

### Relation in an Enclosure

When a surface is completely enclosed, the surface can be subdivided into  $N$  parts having areas  $A_1, A_2, \dots, A_N$ , respectively, and

$$\sum_{j=1}^N F_{i-j} = 1$$

### Black-Body Radiation Exchange

For black surfaces  $A_i$  and  $A_j$  at temperatures  $T_i$  and  $T_j$ , respectively, the net radiative exchange  $q_{ij}$  can be expressed as

$$q_{ij} = A_i F_{i-j} \sigma (T_i^4 - T_j^4)$$

and for a surface completely enclosed and subdivided into  $N$  surfaces maintained at temperatures  $T_1, T_2, \dots, T_N$ , the net radiative heat transfer  $q_i$  to surface area  $A_i$  is

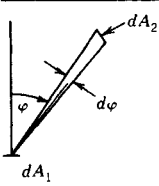
$$q_i = \sum_{j=1}^N A_i F_{i-j} \sigma (T_i^4 - T_j^4) = \sum_{j=1}^N q_{ij}$$

#### 43.4.4 Radiative Exchange among Diffuse-Gray Surfaces in an Enclosure

One method for solving for the radiation exchange between a number of surfaces or bodies is through the use of the *radiosity*  $J$ , defined as the total radiation that leaves a surface per unit time and per unit area. For an opaque surface, this term is defined as

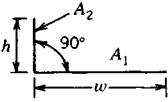
$$J = \varepsilon \sigma T^4 + (1 - \varepsilon)G$$

For an enclosure consisting of  $N$  surfaces, the irradiation on a given surface  $i$  can be expressed as



Area  $dA_1$  of differential width and any length, to infinitely long strip  $dA_2$  of differential width and with parallel generating line to  $dA_1$ :

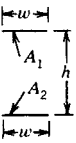
$$dF_{d1-d2} = \frac{\cos \varphi}{2} d\varphi = \frac{1}{2} d(\sin \varphi)$$



Two infinitely long plates of unequal widths  $h$  and  $w$ , having one common edge, and at an angle of  $90^\circ$  to each other:

$$H = \frac{h}{w}$$

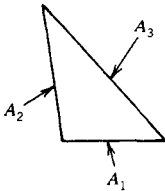
$$F_{1-2} = \frac{1}{2}(1 + H - \sqrt{1 + H^2})$$



Two infinitely long, directly opposed parallel plates of the same finite width:

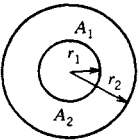
$$H = \frac{h}{w}$$

$$F_{1-2} = F_{2-1} = \sqrt{1 + H^2} - H$$



Infinitely long enclosure formed by three plane areas:

$$F_{1-2} = \frac{A_1 + A_2 - A_3}{2A_1}$$

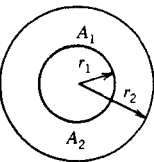


Concentric cylinders of infinite length:

$$F_{1-2} = 1$$

$$F_{2-1} = \frac{r_1}{r_2}$$

$$F_{2-2} = 1 - \frac{r_1}{r_2}$$

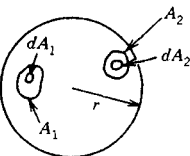


Concentric spheres:

$$F_{1-2} = 1$$

$$F_{2-1} = \left(\frac{r_1}{r_2}\right)^2$$

$$F_{2-2} = 1 - \left(\frac{r_1}{r_2}\right)^2$$



Differential or finite areas on the inside of a spherical cavity:

$$dF_{d1-d2} = dF_{1-d2} = \frac{dA_2}{4\pi r^2}$$

$$F_{d1-2} = F_{1-2} = \frac{A_2}{4\pi r^2}$$

Fig. 43.21 Configuration factors for some simple geometries.<sup>19</sup>

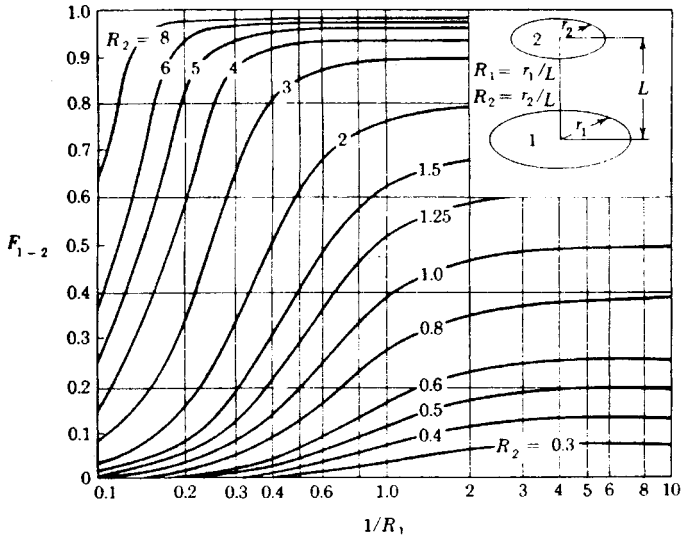


Fig. 43.22 Configuration factor for coaxial parallel circular disks.

$$A_1 F_{1-j} = \sum_{n=1}^N \sum_{m=1}^M A_n F_{i_n-j_m}$$

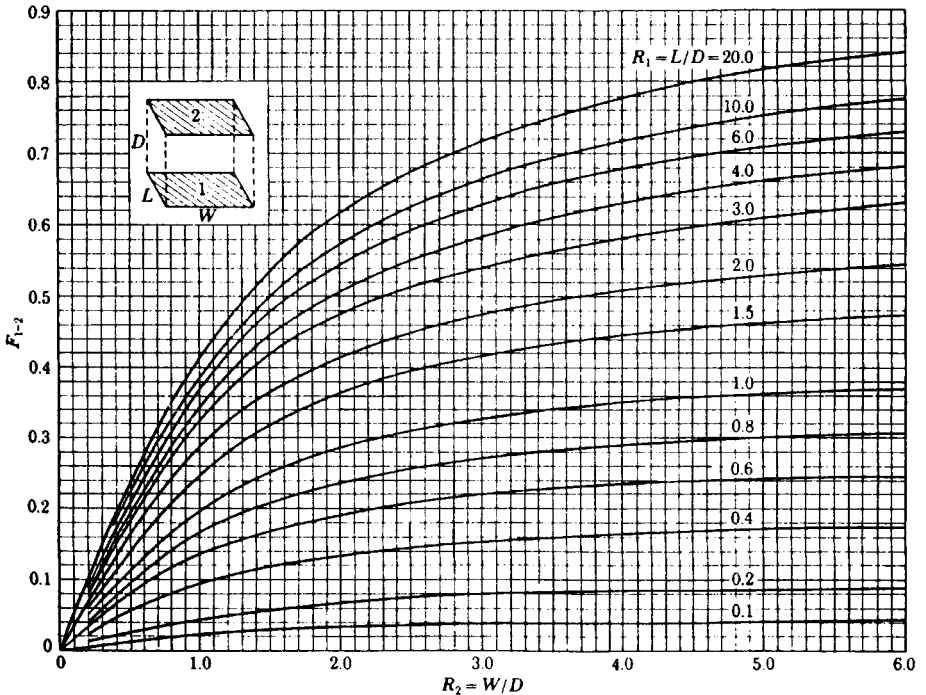


Fig. 43.23 Configuration factor for aligned parallel rectangles.

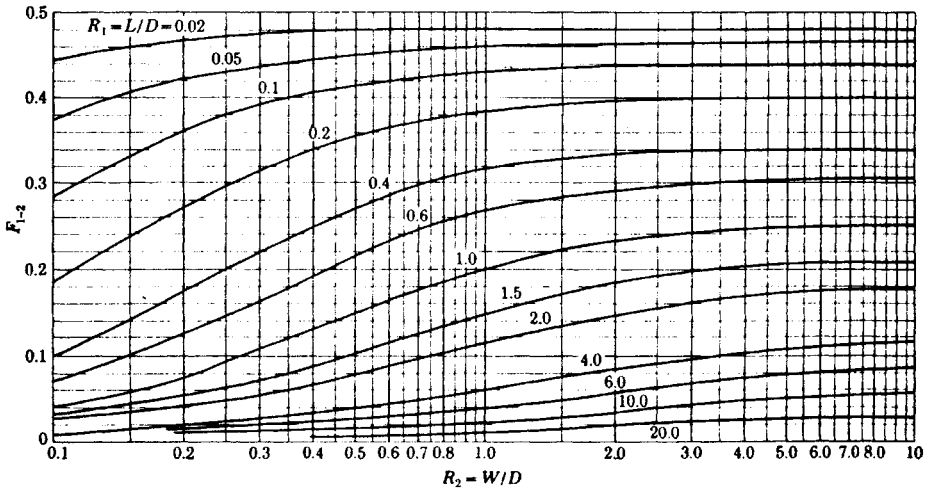
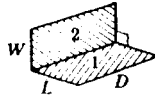


Fig. 43.24 Configuration factor for rectangles with common edge.

$$G_i = \sum_{j=1}^N J_j F_{i-j}$$

and the net radiative heat-transfer rate at given surface  $i$  is

$$q_i = A_i(J_i - G_i) = \frac{\epsilon_i A_i}{1 - \epsilon_i} (\sigma T_i^4 - J_i)$$

For every surface in the enclosure, a uniform temperature or a constant heat transfer rate can be specified. If the surface temperature is given, the heat transfer rate can be determined for that surface and vice versa. Shown below are several specific cases that are commonly encountered

Case I: Temperatures  $T_i$  ( $i = 1, 2, \dots, N$ ) are known for each of the  $N$  surfaces and the values of the radiosity  $J_i$  are solved from the expression

$$\sum_{j=1}^N \{\delta_{ij} - (1 - \epsilon_i) F_{i-j}\} J_j = \epsilon_i \sigma T_i^4 \quad 1 \leq i \leq N$$

The net heat-transfer rate to surface  $i$  can then be determined from the fundamental relationship

$$q_i = A_i \frac{\epsilon_i}{1 - \epsilon_i} (\sigma T_i^4 - J_i) \quad 1 \leq i \leq N$$

where  $\delta_{ij} = 0$  for  $i \neq j$  and  $\delta_{ij} = 1$  for  $i = j$ .

Case II: The heat transfer rates  $q_i$  ( $i = 1, 2, \dots, N$ ) are known for each of the  $N$  surfaces and the values of the radiosity  $J_i$  are determined from

$$\sum_{j=1}^N \{\delta_{ij} - F_{i-j}\} J_j = q_i / A_i \quad 1 \leq i \leq N$$

The surface temperature can then be determined from

$$T_i = \left[ \frac{1}{\sigma} \left( \frac{1 - \epsilon_i}{\epsilon_i} \frac{q_i}{A_i} + J_i \right) \right]^{1/4} \quad 1 \leq i \leq N$$

Case III: The temperatures  $T_i$ , ( $i = 1, \dots, N_i$ ) for  $N_i$  surfaces and heat-transfer rates  $q_i$  ( $i = N_i + 1, \dots, N$ ) for  $(N - N_i)$  surfaces are known and the radiosities are determined by

$$\sum_{j=1}^N \{\delta_{ij} - (1 - \epsilon_i)F_{i-j}\} J_j = \epsilon_i \alpha T_i^4 \quad 1 \leq i \leq N_i$$

$$\sum_{j=1}^N \{\delta_{ij} - F_{i-j}\} J_j = \frac{q_i}{A_i} \quad N_i + 1 \leq i \leq N$$

The net heat-transfer rates and temperatures can be found as

$$q_i = A_i \frac{\epsilon_i}{1 - \epsilon_i} (\sigma T_i^4 - J_i) \quad 1 \leq i \leq N_i$$

$$T_i = \left[ \frac{1}{\sigma} \left( \frac{1 - \epsilon_i}{\epsilon_i} \frac{q_i}{A_i} + J_i \right) \right]^{1/4} \quad N_i + 1 \leq i \leq N$$

### Two Diffuse-Gray Surfaces Forming an Enclosure

The net radiative exchange  $q_{12}$  for two diffuse-gray surfaces forming an enclosure is shown in Table 43.20 for several simple geometries.

#### Radiation Shields

Often, in practice, it is desirable to reduce the radiation heat transfer between two surfaces. This can be accomplished by placing a highly reflective surface between the two surfaces. For this configuration, the ratio of the net radiative exchange with the shield to that without the shield can be expressed by the relationship

$$\frac{q_{12} \text{ with shield}}{q_{12} \text{ without shield}} = \frac{1}{1 + \chi}$$


Values for this ratio  $\chi$  for shields between parallel plates, concentric cylinders, and concentric spheres

**Table 43.20 Net Radiative Exchange between Two Surfaces Forming an Enclosure**

*Large (Infinite) Parallel Planes*

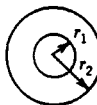
$$\frac{A_1, T_1, \epsilon_1}{A_2, T_2, \epsilon_2} \quad A_1 = A_2 = A \quad q_{12} = \frac{A\sigma(T_1^4 - T_2^4)}{\frac{1}{\epsilon_1} + \frac{1}{\epsilon_2} - 1}$$

*Long (Infinite) Concentric Cylinders*



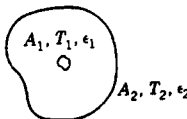
$$\frac{A_1}{A_2} = \frac{r_1}{r_2} \quad q_{12} = \frac{\sigma A_1 (T_1^4 - T_2^4)}{\frac{1}{\epsilon_1} + \frac{1 - \epsilon_2}{\epsilon_2} \left( \frac{r_1}{r_2} \right)}$$

*Concentric Sphere*



$$\frac{A_1}{A_2} = \frac{r_1^2}{r_2^2} \quad q_{12} = \frac{\sigma A_1 (T_1^4 - T_2^4)}{\frac{1}{\epsilon_1} + \frac{1 - \epsilon_2}{\epsilon_2} \left( \frac{r_1}{r_2} \right)^2}$$

*Small Convex Object in a Large Cavity*



$$\frac{A_1}{A_2} \approx 0 \quad q_{12} = \sigma A_1 \epsilon_1 (T_1^4 - T_2^4)$$

are summarized in Table 43.21. For the special case of parallel plates involving more than one or  $N$  shields, where all of the emissivities are equal, the value of  $\chi$  equals  $N$ .

**Radiation Heat-Transfer Coefficient**

The rate at which radiation heat transfer occurs can be expressed in a form similar to Fourier’s law or Newton’s law of cooling by expressing it in terms of the temperature difference  $T_1 - T_2$  or as

$$q = h_r A(T_1 - T_2)$$

where  $h_r$  is the radiation heat-transfer coefficient or *radiation film coefficient*. For the case of radiation between two large parallel plates with emissivities, respectively, of  $\epsilon_1$  and  $\epsilon_2$ ,

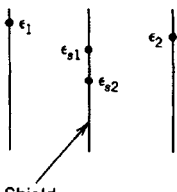
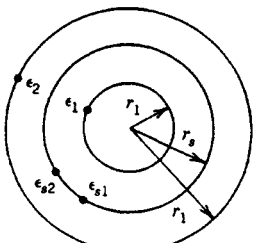
$$h_r = \frac{(T_1^4 - T_2^4)}{(T_1 - T_2) \left( \frac{1}{\epsilon_1} + \frac{1}{\epsilon_2} - 1 \right)}$$

**43.4.5 Thermal Radiation Properties of Gases**

All of the previous expressions assumed that the medium present between the surfaces did not affect the radiation exchange. In reality, gases such as air, oxygen ( $O_2$ ), hydrogen ( $H_2$ ), and nitrogen ( $N_2$ ) have a symmetrical molecular structure and neither emit nor absorb radiation at low to moderate temperatures. Hence, for most engineering applications, such *non-participating gases* can be ignored. However, polyatomic gases, such as water vapor ( $H_2O$ ), carbon dioxide ( $CO_2$ ), carbon monoxide ( $CO$ ), sulfur dioxide ( $SO_2$ ), and various hydrocarbons, emit and absorb significant amounts of radiation. These *participating gases* absorb and emit radiation in limited spectral ranges, referred to as spectral *bands*. In calculating the emitted or absorbed radiation for a gas layer, its thickness, shape, surface area, pressure, and temperature distribution must be considered. Although a precise method for calculating the effect of these participating media is quite complex, an approximate method developed by Hottel<sup>21</sup> will yield results that are reasonably accurate.

The effective total emissivities of carbon dioxide and water vapor are a function of the temperature and the product of the partial pressure and the mean beam length of the substance, as indicated in Figs. 43.24 and 43.25, respectively. The *mean beam length*  $L_e$  is the characteristic length that corresponds to the radius of a hemisphere of gas, such that the energy flux radiated to the center of the base is equal to the average flux radiated to the area of interest by the actual gas volume. Table 43.22 lists the mean beam lengths of several simple shapes. For a geometry for which  $L_e$  has not been determined, it is generally approximated by  $L_e = 3.6V/A$  for an entire gas volume  $V$  radiating to its entire boundary surface  $A$ . The data in Figs. 43.25 and 43.26 were obtained for a total pressure of 1

**Table 43.21 Values of  $X$  for Radiative Shields**

Geometry	$X$	
	$\frac{1}{\epsilon_{s1}} + \frac{1}{\epsilon_{s2}} - 1$ $\frac{1}{\epsilon_1} + \frac{1}{\epsilon_2} - 1$	Infinitely long parallel plates
	$\left( \frac{r_1}{r_2} \right)^2 \left( \frac{1}{\epsilon_{s1}} + \frac{1}{\epsilon_{s2}} - 1 \right)$ $\frac{1}{\epsilon_1} + \left( \frac{1}{\epsilon_2} - 1 \right) \left( \frac{r_1}{r_2} \right)^2$	$n = 1$ for infinitely long concentric cylinders $n = 2$ for concentric spheres



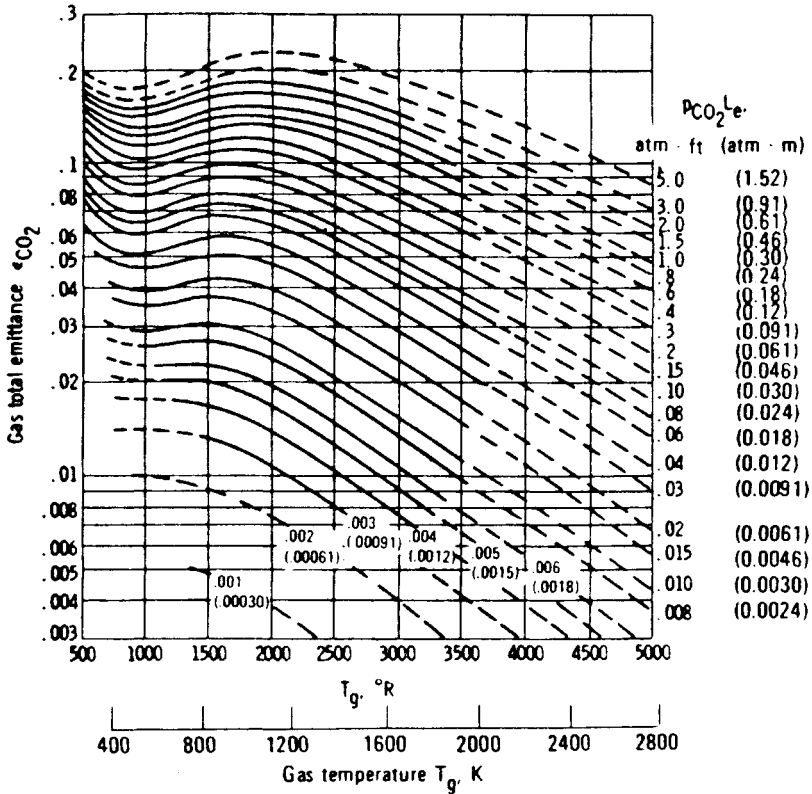


Fig. 43.25 Total emissivity of CO<sub>2</sub> in a mixture having a total pressure of 1 atm. From Ref. 21. (Used with the permission of McGraw-Hill Book Company.)

atm and zero partial pressure of the water vapor. For other total and partial pressures, the emissivities are corrected by multiplying  $C_{CO_2}$  (Fig. 43.27) and  $C_{H_2O}$  (Fig. 43.28), respectively, to  $\epsilon_{CO_2}$  and  $\epsilon_{H_2O}$ , which are found from Figs. 43.25 and 43.26.

These results can be applied when water vapor or carbon dioxide appear separately or in a mixture with other non-participating gases. For mixtures of CO<sub>2</sub> and water vapor in a non-participating gas, the total emissivity of the mixture  $\epsilon_g$  can be estimated from the expression

$$\epsilon_g = C_{CO_2} \epsilon_{CO_2} + C_{H_2O} \epsilon_{H_2O} - \Delta \epsilon$$

where  $\Delta \epsilon$  is a correction factor given in Fig. 43.29.

**Radiative Exchange between Gas Volume and Black Enclosure of Uniform Temperature**

When radiative energy is exchanged between a gas volume and a black enclosure, the exchange per unit area  $q''$  for a gas volume at uniform temperature  $T_g$  and a uniform wall temperature  $T_w$  is given by

$$q'' = \epsilon_g(T_g) \sigma T_g^4 - \alpha_g(T_w) \sigma T_w^4$$

where  $\epsilon_g(T_g)$  is the gas emissivity at a temperature  $T_g$  and  $\alpha_g(T_w)$  is the absorptivity of gas for the radiation from the black enclosure at  $T_w$ . As a result of the nature of the band structure of the gas, the absorptivity  $\alpha_g$  for black radiation at a temperature  $T_w$  is different from the emissivity  $\epsilon_g$  at a gas temperature of  $T_g$ . When a mixture of carbon dioxide and water vapor is present, the empirical expression for  $\alpha_g$  is

$$\alpha_g = \alpha_{CO_2} + \alpha_{H_2O} - \Delta \alpha$$

where

**Table 43.22 Mean Beam Length<sup>a</sup>**

Geometry of Gas Volume	Characteristic Length	$L_e$
Hemisphere radiating to element at center of base	Radius $R$	$R$
Sphere radiating to its surface	Diameter $D$	$0.65D$
Circular cylinder of infinite height radiating to concave bounding surface	Diameter $D$	$0.95D$
Circular cylinder of semi-infinite height radiating to:		
Element at center of base	Diameter $D$	$0.90D$
Entire base	Diameter $D$	$0.65D$
Circular cylinder of height equal to diameter radiating to:		
Element at center of base	Diameter $D$	$0.71D$
Entire surface	Diameter $D$	$0.60D$
Circular cylinder of height equal to two diameters radiating to:		
Plane end	Diameter $D$	$0.60D$
Concave surface	Diameter $D$	$0.76D$
Entire surface	Diameter $D$	$0.73D$
Infinite slab of gas radiating to:		
Element on one face	Slab thickness $D$	$1.8D$
Both bounding planes	Slab thickness $D$	$1.8D$
Cube radiating to a face	Edge $X$	$0.6X$
Gas volume surrounding an infinite tube bundle and radiating to a single tube:		
Equilateral triangular array:	Tube diameter $D$ and spacing between tube centers, $S$	$3.0(S - D)$
$S = 2D$		$3.8(S - D)$
$S = 3D$		
Square array:		$3.5(S - D)$
$S = 2D$		

<sup>a</sup>Adapted from Ref. 19.

$$\alpha_{\text{CO}_2} = C_{\text{CO}_2} \epsilon'_{\text{CO}_2} \left( \frac{T_g}{T_w} \right)^{0.65}$$

$$\alpha_{\text{H}_2\text{O}} = C_{\text{H}_2\text{O}} \epsilon'_{\text{H}_2\text{O}} \left( \frac{T_g}{T_w} \right)^{0.45}$$

where  $\Delta\alpha = \Delta\epsilon$  and all properties are evaluated at  $T_w$ . In this expression, the values of  $\epsilon'_{\text{CO}_2}$  and  $\epsilon'_{\text{H}_2\text{O}}$  can be found from Figs. 43.25 and 43.26 using an abscissa of  $T_w$ , but substituting the parameters  $p_{\text{CO}_2} L_e T_w / T_g$  and  $p_{\text{H}_2\text{O}} L_e T_w / T_g$  for  $p_{\text{CO}_2} L_e$  and  $p_{\text{H}_2\text{O}} L_e$ , respectively.

### Radiative Exchange between a Gray Enclosure and a Gas Volume

When the emissivity of the enclosure  $\epsilon_w$  is larger than 0.8, the rate of heat transfer may be approximated by

$$q_{\text{gray}} = \left( \frac{\epsilon_w + 1}{2} \right) q_{\text{black}}$$

where  $q_{\text{gray}}$  is the heat-transfer rate for gray enclosure and  $q_{\text{black}}$  is that for black enclosure. For values of  $\epsilon_w < 0.8$ , the band structures of the participating gas must be taken into account for heat-transfer calculations.

## 43.5 BOILING AND CONDENSATION HEAT TRANSFER

Boiling and condensation are both forms of convection in which the fluid medium is undergoing a change of phase. When a liquid comes into contact with a solid surface maintained at a temperature above the saturation temperature of the liquid, the liquid may vaporize, resulting in boiling. This process is always accompanied by a change of phase from the liquid to the vapor state and results

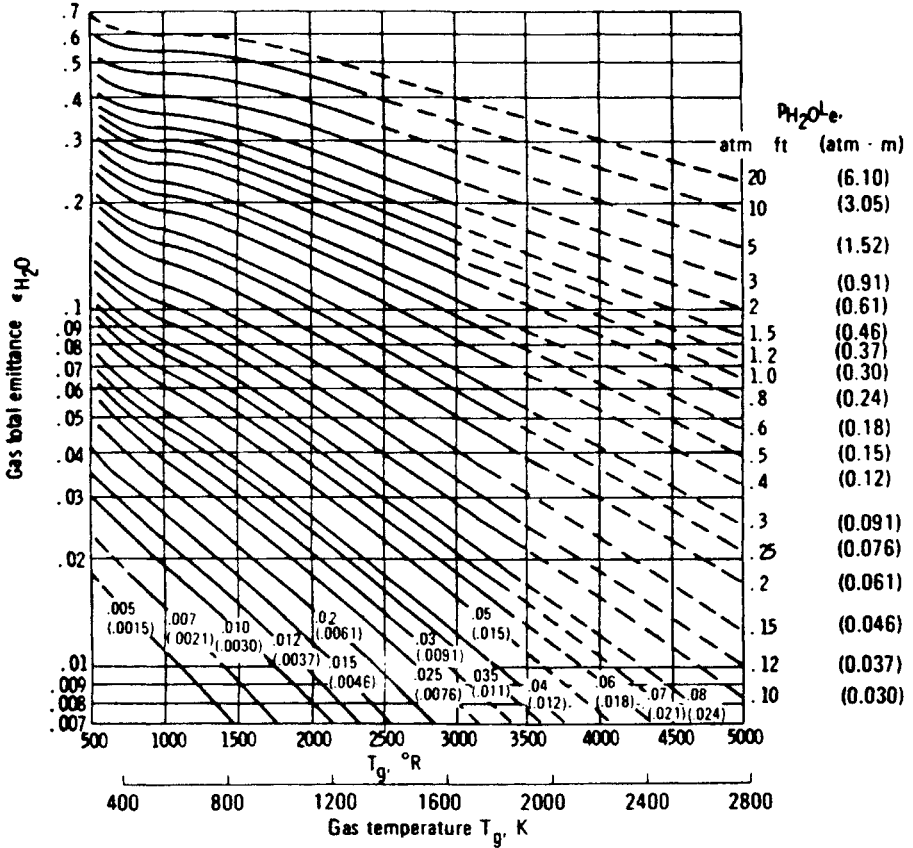


Fig. 43.26 Total emissivity of  $H_2O$  at 1 atm total pressure and zero partial pressure. (From Ref. 21. Used with the permission of McGraw-Hill Book Company.)

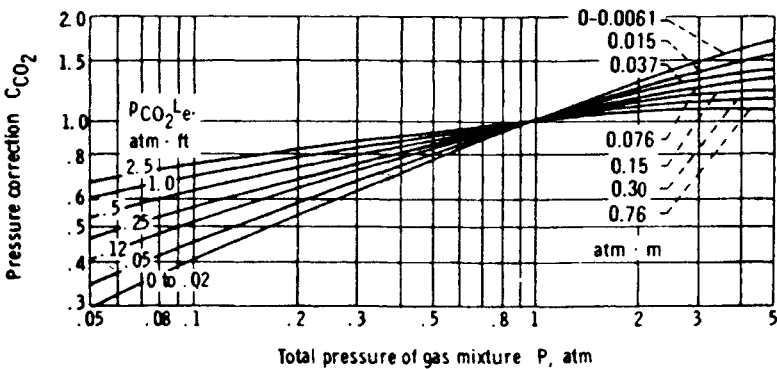
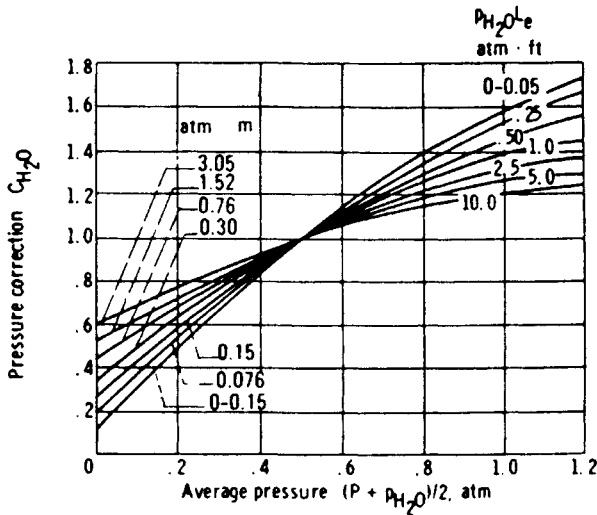


Fig. 43.27 Pressure correction for  $CO_2$  total emissivity for values of  $P$  other than 1 atm. Adapted from Ref. 21. (Used with the permission of McGraw-Hill Book Company.)



**Fig. 43.28** Pressure correction for water vapor total emissivity for values of  $P_{H_2O}$  and  $P$  other than 0 and 1 atm. Adapted from Ref. 21. (Used with the permission of McGraw-Hill Book Company.)

in large rates of heat transfer from the solid surface, due to the latent heat of vaporization of the liquid. The process of condensation is usually accomplished by allowing the vapor to come into contact with a surface at a temperature below the saturation temperature of the vapor, in which case the liquid undergoes a change in state from the vapor state to the liquid state, giving up the latent heat of vaporization.

The heat-transfer coefficients for condensation and boiling are generally larger than that for convection without phase change, sometimes by as much as several orders of magnitude. Application of boiling and condensation heat transfer may be seen in a closed-loop power cycle or in a device referred to as a *heat pipe*, which will be discussed in the following section. In power cycles, the liquid is vaporized in a boiler at high pressure and temperature. After producing work by means of expansion through a turbine, the vapor is condensed to the liquid state in a condenser and then returned to the boiler, where the cycle is repeated.

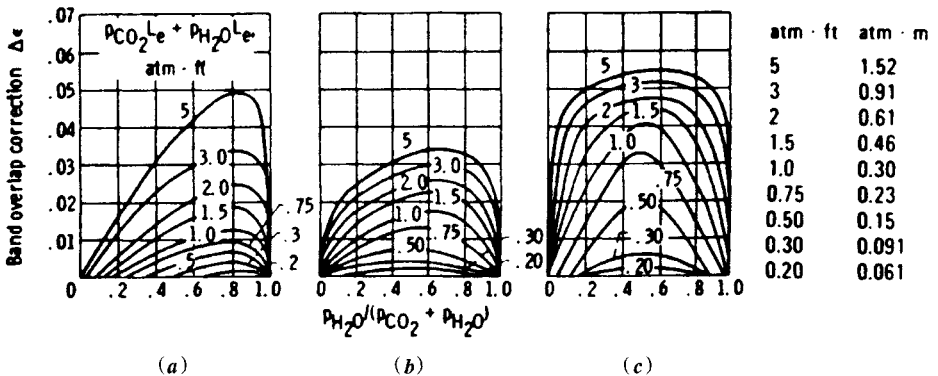


**Fig. 43.29** Correction on total emissivity for band overlap when both  $CO_2$  and water vapor are present: (a) gas temperature  $T_g = 400$  K ( $720^\circ R$ ); (b) gas temperature  $T_g = 810$  K ( $1460^\circ R$ ); (c) gas temperature  $T_g = 1200$  K ( $2160^\circ R$ ). Adapted from Ref. 21. (Used with the permission of McGraw-Hill Book Company.)

### 43.5.1 Boiling

The formation of vapor bubbles on a hot surface in contact with a quiescent liquid without external agitation it is called *pool boiling*. This differs from *forced-convection boiling*, in which forced convection occurs simultaneously with boiling. When the temperature of the liquid is below the saturation temperature, the process is referred to as *subcooled boiling*. When the liquid temperature is maintained or exceeds the saturation temperature, the process is referred to as *saturated or saturation boiling*. Figure 43.30 depicts the surface heat flux  $q''$  as a function of the excess temperature  $\delta T_e = T_s - T_{sat}$ , for typical pool boiling of water using an electrically heated wire. In the region  $0 < \Delta T_e < \Delta T_{e,A}$ , bubbles occur only on selected spots of the heating surface and the heat transfer occurs primarily through free convection. This process is called *free convection boiling*. When  $\Delta T_{e,A} < \Delta T_e < \Delta T_{e,C}$ , the heated surface is densely populated with bubbles and the bubble separation and eventual rise due to buoyancy induces a considerable stirring action in the fluid near the surface. This stirring action substantially increases the heat transfer from the solid surface. This process or region of the curve is referred to as *nucleate boiling*. When the excess temperature is raised to  $\Delta T_{e,C}$ , the heat flux reaches a maximum value and further increases in the temperature will result in a decrease in the heat flux. The point at which the heat flux is at a maximum value is called the *critical heat flux*.

*Film boiling* occurs in the region where  $\Delta T_e > \Delta T_{e,D}$ , and the entire heating surface is covered by a vapor film. In this region, the heat transfer to the liquid is caused by conduction and radiation through the vapor. Between points C and D, the heat flux decreases with increasing  $\Delta T_e$ . In this region, part of the surface is covered by bubbles and part by a film. The vaporization in this region is called *transition boiling* or *partial film boiling*. The point of maximum heat flux, point C, is called the *burnout point* or the *Liedenfrost point*. Although it is desirable to operate vapor generators at heat fluxes close to  $q''_C$ , to permit the maximum use of the surface area, in most engineering applications, it is necessary to control the heat flux and great care is taken to avoid reaching this point. The primary reason for this is that, as illustrated, when the heat flux is increased gradually, the temperature rises steadily until point C is reached. Any increase of heat flux beyond the value of  $q''_C$ , however, will dramatically change the surface temperature to  $T_s = T_{sat} + T_{e,E}$ , typically exceeding the solid melting point and leading to failure of the material in which the liquid is held or from which the heater is fabricated.

#### Nucleate Pool Boiling

The heat flux data are best correlated by<sup>25</sup>

$$q'' = \mu_l h_g \left( \frac{g(\rho_l - \rho_v)}{g_c \sigma} \right)^{1/2} \left( \frac{c_{p,l} \Delta T_e}{Ch_{fg} Pr_l^{1.7}} \right)^3$$

where the subscripts  $l$  and  $v$  denote saturated liquid and vapor, respectively. The surface tension of the liquid is  $\sigma$  (N/m). The quantity  $g_c$  is the proportionality constant equal to  $1 \text{ kg} \cdot \text{m}/\text{N} \cdot \text{sec}^2$ . The quantity  $g$  is the local gravitational acceleration in  $\text{m}/\text{sec}^2$ . The values of  $C$  are given in Table 43.24. The above equation may be applied to different geometries such as plates, wire, or cylinders.

The *critical heat flux* (point C of Fig. 43.30) is given by<sup>27</sup>

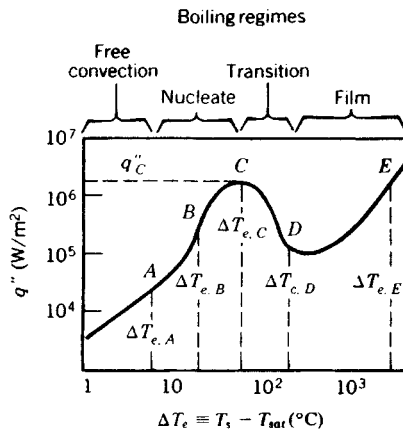


Fig. 43.30 Typical boiling curve for a wire in a pool of water at atmospheric pressure.

**Table 43.23 Thermophysical Properties of Saturated Water**

Temperature $T$ (K)	Pressure $P$ (bar) <sup>a</sup>	Specific Volume (m <sup>3</sup> /kg)		Heat of Vaporization $h_{fg}$ (kJ/kg)	Specific Heat (kJ/kg · K)		Viscosity (N · sec/m <sup>2</sup> )		Thermal Conductivity (W/m · K)		Prandtl Number		Surface Tension $\sigma_f \times 10^3$ (N/m)	Expansion Coefficient $\beta_1 \times 10^6$ (K <sup>-1</sup> )
		$v_f \times 10^3$	$v_u$		$C_{p,l}$	$C_{p,u}$	$\mu_l \times 10^6$	$\mu_v \times 10^3$	$k_l \times 10^3$	$k_v \times 10^3$	$Pr_l$	$Pr_v$		
273.15	0.00611	1.000	206.3	2502	4.217	1.854	1750	8.02	659	18.2	12.99	0.815	75.5	-68.05
300	0.03531	1.003	39.13	2438	4.179	1.872	855	9.09	613	19.6	5.83	0.857	71.7	276.1
320	0.1053	1.011	13.98	2390	4.180	1.895	577	9.89	640	21.0	3.77	0.894	68.3	436.7
340	0.2713	1.021	5.74	2342	4.188	1.930	420	10.69	660	22.3	2.66	0.925	64.9	566.0
360	0.6209	1.034	2.645	2291	4.203	1.983	324	11.49	674	23.7	2.02	0.960	61.4	697.9
380	1.2869	1.049	1.337	2239	4.226	2.057	260	12.29	683	25.4	1.61	0.999	57.6	788
400	2.455	1.067	0.731	2183	4.256	2.158	217	13.05	688	27.2	1.34	1.033	63.6	896
450	9.319	1.123	0.208	2024	4.40	2.56	152	14.85	678	33.1	0.99	1.14	42.9	
500	26.40	1.203	0.0766	1825	4.66	3.27	118	16.59	642	42.3	0.86	1.28	31.6	
550	61.19	1.323	0.0317	1564	5.24	4.64	97	18.6	580	58.3	0.87	1.47	19.7	
600	123.5	1.541	0.0137	1176	7.00	8.75	81	22.7	497	92.9	1.14	2.15	8.4	
647.3	221.2	3.170	0.0032	0	$\infty$	$\infty$	45	45	238	238	$\infty$	$\infty$	0.0	

**Table 43.24 Values of the Constant C for Various Liquid–Surface Combinations<sup>a</sup>**

Fluid-Heating Surface Combinations	C
Water with polished copper, platinum, or mechanically polished stainless steel	0.0130
Water with brass or nickel	0.006
Water with ground and polished stainless steel	0.008
Water with Teflon-plated stainless steel	0.008

<sup>a</sup>Adapted from Ref. 26.

$$q_c'' = \frac{\pi}{24} h_{fg} \rho_v \left( \frac{\sigma g g_c (\rho_l - \rho_v)}{\rho_v^2} \right)^{0.25} \left( 1 + \frac{\rho_v}{\rho_l} \right)^{0.5}$$

For a water–steel combination,  $q_c'' \approx 1290 \text{ KW/m}^2$  and  $\Delta T_{e,c} \approx 30^\circ\text{C}$ . For water–chrome-plated copper,  $q_c'' \approx 940\text{--}1260 \text{ KW/m}^2$  and  $\Delta T_{e,c} \approx 23\text{--}28^\circ\text{C}$ .

### Film Pool Boiling

The heat transfer from a surface to a liquid is due to both convection and radiation. A total heat-transfer coefficient is defined by the combination of convection and radiation heat-transfer coefficients of the following form<sup>28</sup> for the outside surfaces of horizontal tubes:

$$h^{4/3} = h_c^{4/3} + h_r h^{1/3}$$

where

$$h_c = 0.62 \left( \frac{k_v^3 \rho_v (\rho_l - \rho_v) g (h_{fg} + 0.4 c_{p,v} \Delta T_e)}{\mu_v D \Delta T_e} \right)^{1/4}$$

and

$$h_r = \frac{5.73 \times 10^{-8} \varepsilon (T_s^4 - T_{sat}^4)}{T_s - T_{sat}}$$

The vapor properties are evaluated at the film temperature  $T_f = (T_s + T_{sat})/2$ . The temperatures  $T_s$  and  $T_{sat}$  are in Kelvins for the evaluation of  $h_r$ . The emissivity of the metallic solids can be found from Table 43.17. Note that  $q = hA(T_s - T_{sat})$ .

### Nucleate Boiling in Forced Convection

The total heat-transfer rate can be obtained by simply superimposing the heat transfer due to nucleate boiling and forced convection:

$$q'' = q''_{\text{boiling}} + q''_{\text{forced convection}}$$

For forced convection, it is recommended that the coefficient 0.023 be replaced by 0.014 in the Dittus–Boelter equation (Section 43.2.1). The above equation is generally applicable to forced convection where the bulk liquid temperature is subcooled (*local forced convection boiling*).

### Simplified Relations for Boiling in Water

For *nucleate boiling*,<sup>29</sup>

$$h = C(\Delta T_e)^n \left( \frac{p}{p_a} \right)^{0.4}$$

where  $p$  and  $p_a$  are, respectively, the system pressure and standard atmospheric pressure. The constants  $C$  and  $n$  are listed in Table 43.25.

For *local forced convection boiling inside vertical tubes*, valid over a pressure range of 5–170 atm (Ref. 29, Vol. 2, p. 584),

**Table 43.25 Values of  $C$  and  $n$  for Simplified Relations for Boiling in Water<sup>a</sup>**

Surface	$q''$ (KW/m <sup>2</sup> )	$C$	$n$
Horizontal	$q'' < 16$	1042	1/3
	$16 < q'' < 240$	5.56	3
Vertical	$q'' < 3$	5.7	1/7
	$3 < q'' < 63$	7.96	3

<sup>a</sup>Adapted from Ref. 29.

$$h = 2.54(\Delta T_e)^3 e^{p/1.551}$$

where  $h$  has the unit  $W/m^2 \cdot ^\circ C$ ,  $\Delta T_e$  is in  $^\circ C$ , and  $p$  is the pressure in  $10^6$  N/m<sup>3</sup>.

### 43.5.2 Condensation

Depending on the surface conditions, the condensation may be a *film condensation* or a *dropwise condensation*. Film condensation usually occurs when a vapor, relatively free of impurities, is allowed to condense on a clean, uncontaminated surface. Dropwise condensation occurs on highly polished surfaces or on surfaces coated with substances that inhibit wetting. The condensate provides a resistance to heat transfer between the vapor and the surface. Therefore, it is desirable to use short vertical surfaces or horizontal cylinders to prevent the condensate from growing too thick. The heat-transfer rate for dropwise condensation is usually an order of magnitude larger than that for film condensation under similar conditions. Silicones, Teflon, and certain fatty acids can be used to coat the surfaces to promote dropwise condensation. However, such coatings may lose their effectiveness owing to oxidation or outright removal. Thus, except under carefully controlled conditions, film condensation may be expected to occur in most instances, and the condenser design calculations are often based on the assumption of film condensation.

For condensation on a surface at temperature  $T_s$ , the total heat-transfer rate to the surface is given by  $q = \bar{h}_L A (T_{sat} - T_s)$ , where  $T_{sat}$  is the saturation temperature of the vapor. The mass flow rate is determined by  $\dot{m} = q/h'_{fg}$ ;  $h'_{fg}$  is the latent heat of vaporization of the fluid (see Table 43.23 for saturated water). Correlations are based on the evaluation of liquid properties at  $T_f = (T_s + T_{sat})/2$  except  $h'_{fg}$ , which is to be taken at  $T_{sat}$ .

#### Film Condensation on a Vertical Plate

The Reynolds number for *condensate flow* is defined by  $Re_\Phi = \rho_l V_m D_h / \mu_l$ , where  $\rho_l$  and  $\mu_l$  are the density and viscosity of the liquid,  $V_m$  is the average velocity of the condensate, and  $D_h$  is the hydraulic diameter defined by  $D_h = 4 \times$  condensate film cross-sectional area/wetted perimeter. For the condensation on a vertical plate,  $Re_\Gamma = 4\Gamma/\mu_l$ , where  $\Gamma$  is the mass flow rate of condensate per unit width evaluated at the lowest point on the condensing surface. The condensate flow is generally considered to be laminar for  $Re_\Gamma < 1800$  and turbulent for  $Re_\Gamma > 1800$ . The average Nusselt number is given by<sup>14</sup>

$$\bar{Nu}_L = 1.13 \left[ \frac{g\rho_l(\rho_l - \rho_v)h'_{fg}L^3}{\mu_l k_f (T_{sat} - T_s)} \right]^{0.25} \quad \text{for } Re_\Gamma < 1800$$

$$\bar{Nu}_L = 0.0077 \left[ \frac{g\rho_l(\rho_l - \rho_v)L^3}{\mu_l^2} \right]^{1/3} Re_\Gamma^{0.4} \quad \text{for } Re_\Gamma > 1800$$

#### Film Condensation on the Outside of Horizontal Tubes and Tube Banks

$$\bar{Nu}_D = 0.725 \left[ \frac{g\rho_l(\rho_l - \rho_v)h'_{fg}D^3}{N\mu_l k_f (T_{sat} - T_s)} \right]^{0.25}$$

where  $N$  is the number of horizontal tubes placed one above the other;  $N = 1$  for a single tube.<sup>23</sup>

#### Film Condensation Inside Horizontal Tubes

For low vapor velocities such that  $Re_D$  based on the vapor velocities at the pipe inlet is less than 3500,<sup>23</sup>

$$\bar{Nu}_D = 0.555 \left[ \frac{g\rho_l(\rho_l - \rho_v)h'_{fg}D^3}{\mu_l k_f (T_{sat} - T_s)} \right]^{0.25}$$

where  $h'_{fg} + \frac{3}{8}C_{p,f}(T_{sat} - T_s)$ .



For higher flow rates,<sup>24</sup>  $Re_G > 5 \times 10^4$ ,

$$\overline{Nu}_D = 0.0265 Re_G^{0.8} Pr^{1/3}$$

where the Reynolds number  $Re_G = GD/\mu_l$  is based on the equivalent mass velocity  $G = G_l + G_v(\rho_l/\rho_v)^{0.5}$ . The mass velocity for the liquid  $G_l$  and for vapor  $G_v$  are calculated as if each occupied the entire flow area alone.

### The Effect of Noncondensable Gases

If noncondensable gas such as air is present in a vapor, even in a small amount, the heat transfer coefficient for condensation may be greatly reduced. It has been found that the presence of a few percent of air by volume in steam reduces the coefficient by 50% or more. Therefore, it is desirable in the condenser design to vent the noncondensable gases as much as possible.

### 43.5.3 Heat Pipes

Heat pipes are a two-phase heat transfer device that operate on a closed two-phase cycle<sup>31</sup> and come in a wide variety of sizes and shapes.<sup>31,32</sup> As shown in Fig. 43.31, they typically consist of three distinct regions, the evaporator or heat addition region, the condenser or heat rejection region, and the adiabatic or isothermal region. Heat added to the evaporator region of the container causes the working fluid in the evaporator wicking structure to be vaporized. The high temperature and corresponding high pressure in this region result in flow of the vapor to the other, cooler end of the container, where the vapor condenses, giving up its latent heat of vaporization. The capillary forces existing in the wicking structure then pump the liquid back to the evaporator section. Other similar devices, referred to as *two-phase thermosyphons*, have no wick, and utilize gravitational forces to provide the liquid return. Thus the heat pipe functions as a nearly isothermal device, adjusting the evaporation rate to accommodate a wide range of power inputs, while maintaining a relatively constant source temperature.

### Transport Limitations

The transport capacity of a heat pipe is limited by several important mechanisms, including the capillary wicking, viscous, sonic, entrainment, and boiling limits. The capillary wicking limit and viscous limits deal with the pressure drops occurring in the liquid and vapor phases, respectively. The sonic limit results from the occurrence of choked flow in the vapor passage, while the entrainment limit is due to the high liquid vapor shear forces developed when the vapor passes in counter-flow over the liquid saturated wick. The boiling limit is reached when the heat flux applied in the evap-

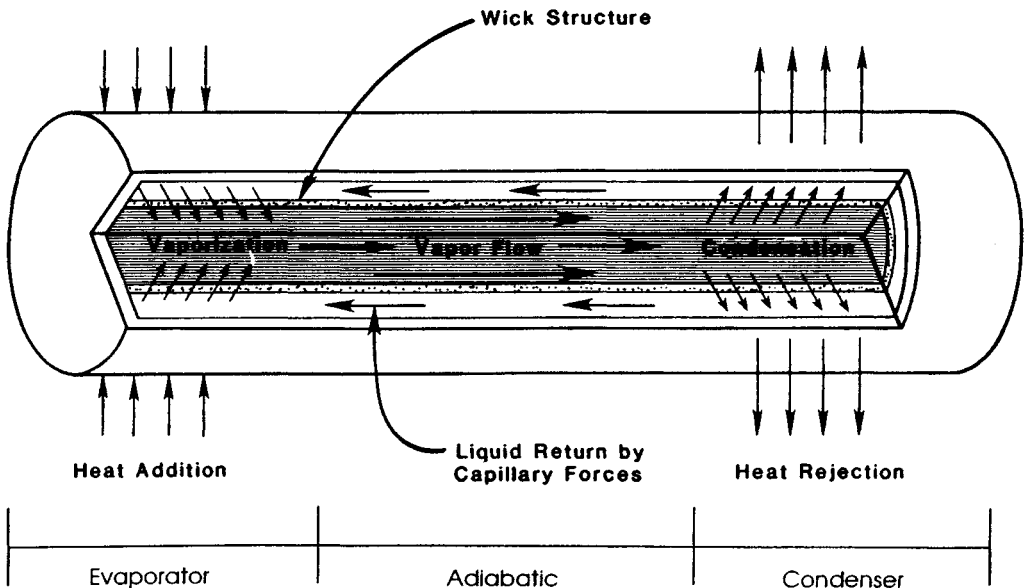


Fig. 43.31 Typical heat pipe construction and operation.<sup>33</sup>

erator portion is high enough that nucleate boiling occurs in the evaporator wick, creating vapor bubbles that partially block the return of fluid.

In order to function properly, the net capillary pressure difference between the condenser and the evaporator in a heat pipe must be greater than the pressure losses throughout the liquid and vapor flow paths. This relationship can be expressed as

$$\Delta P_c \geq \Delta P_+ + \Delta P_- + \Delta P_l + \Delta P_v$$

- where  $\Delta P_c$  = net capillary pressure difference
- $\Delta P_+$  = normal hydrostatic pressure drop
- $\Delta P_-$  = axial hydrostatic pressure drop
- $\Delta P_l$  = viscous pressure drop occurring in the liquid phase
- $\Delta P_v$  = viscous pressure drop occurring in the vapor phase.

If these conditions are not met, the heat pipe is said to have reached the *capillary limitation*.

Expressions for each of these terms have been developed for steady-state operation, and are summarized below.

*Capillary Pressure*

$$\Delta P_{c,m} = \left( \frac{2\sigma}{r_{c,e}} \right)$$

Values for the effective capillary radius  $r_c$  can be found theoretically for simple geometries or experimentally for pores or structures of more complex geometry. Table 43.26 gives values for some common wicking structures.

*Normal and Axial Hydrostatic Pressure Drop*

$$\begin{aligned} \Delta P_+ &= \rho_l g d_v \cos \psi \\ \Delta P_- &= \rho_l g L \sin \psi \end{aligned}$$

In a gravitational environment, the axial hydrostatic pressure term may either assist or hinder the capillary pumping process, depending upon whether the tilt of the heat pipe promotes or hinders the flow of liquid back to the evaporator (i.e., the evaporator lies either below or above the condenser). In a zero-g environment, both this term and the normal hydrostatic pressure drop term can be neglected because of the absence of body forces.

*Liquid Pressure Drop*

$$\Delta P_l = \left( \frac{\mu_l}{KA_w h_{fg} \rho_l} \right) L_{eff} q$$

where  $L_{eff}$  = the effective heat pipe length, defined as

**Table 43.26 Expressions for the Effective Capillary Radius for Several Wick Structures**

Structure	$r_c$	Data
Circular cylinder (artery or tunnel wick)	$r$	$r$ = radius of liquid flow passage
Rectangular groove	$\omega$	$\omega$ = groove width
Triangular groove	$\omega / \cos \beta$	$\omega$ = groove width $\beta$ = half-included angle
Parallel wires	$\omega$	$\omega$ = wire spacing
Wire screens	$(\omega + d_w) / 2 = \frac{1}{2}N$	$d$ = wire diameter $N$ = screen mesh number $\omega$ = wire spacing
Packed spheres	$0.41 r_s$	$r_s$ = sphere radius

$$L_{\text{eff}} = 0.5L_e + L_a + 0.5L_c$$

and  $K$  is the liquid permeability as shown in Table 43.26.

### Vapor Pressure Drop

$$\Delta P_v = \left( \frac{C(f_v Re_v) \mu_v}{2(r_{h,v})^2 A_v \rho_v h_{fg}} \right) L_{\text{eff}} q$$

Although during steady-state operation the liquid flow regime is always laminar, the vapor flow may be either laminar or turbulent. It is therefore necessary to determine the vapor flow regime as a function of the heat flux. This can be accomplished by evaluating the local axial Reynolds and Mach numbers and substituting the values as shown below:

$$Re_v < 2300, Ma_v < 0.2$$

$$(f_v Re_v) = 16$$

$$C = 1.00$$

$$Re_v < 2300, Ma_v > 0.2$$

$$(f_v Re_v) = 16$$

$$C = \left[ 1 + \left( \frac{\gamma_v - 1}{2} \right) Ma_v^2 \right]^{-1/2}$$

$$Re_v > 2300, Ma_v < 0.2$$

$$(f_v Re_v) = 0.038 \left( \frac{2(r_{h,v})q}{A_v \mu_v h_{fg}} \right)^{3/4}$$

$$C = 1.00$$

$$Re_v > 2300, Ma_v > 0.2$$

$$(f_v Re_v) = 0.038 \left( \frac{2(r_{h,v})q}{A_v \mu_v h_{fg}} \right)^{3/4}$$

$$C = \left[ 1 + \left( \frac{\gamma_v - 1}{2} \right) Ma_v^2 \right]^{-1/2}$$

Since the equations used to evaluate both the Reynolds number and the Mach number are functions of the heat transport capacity, it is necessary to first assume the conditions of the vapor flow. Using these assumptions, the maximum heat transport capacity  $q_{c,m}$  can be determined by substituting the values of the individual pressure drops into equation (1) and solving for  $q_{c,m}$ . Once the value of  $q_{c,m}$  is known, it can then be substituted into the expressions for the vapor Reynolds number and Mach number to determine the accuracy of the original assumption. Using this iterative approach, accurate values for the capillary limitation as a function of the operating temperature can be determined in units of watt-m or watts for  $(qL)_{c,m}$  and  $q_{c,m}$  respectively.

The *viscous limitation* in heat pipes occurs when the viscous forces within the vapor region are dominant and limit the heat pipe operation. The expression

$$\frac{\Delta P_v}{P_v} < 0.1$$

can be used to determine when this limit might be of a concern. Due to the operating temperature range, this limitation will normally be of little consequence in the design of heat pipes for use in the thermal control of electronic components and devices, but may be important in liquid metal heat pipes.

The *sonic limitation* in heat pipes is analogous to the sonic limitation in a converging-diverging nozzle and can be determined from

$$q_{s,m} = A_v \rho_v h_{fg} \left( \frac{\gamma_v R_v T_v}{2(\gamma_v + 1)} \right)^{1/2}$$

where  $T_v$  is the mean vapor temperature within the heat pipe.

Since the liquid and vapor flow in opposite directions in a heat pipe, at high enough vapor velocities, liquid droplets may be picked up or entrained in the vapor flow. This entrainment results

in excess liquid accumulation in the condenser and, hence, dryout of the evaporator wick. Using the Weber number,  $We$ , defined as the ratio of the viscous shear force to the force resulting from the liquid surface tension, an expression for the *entrainment limit* can be found as

$$q_{e,m} = A_v h_{fg} \left( \frac{\sigma \rho_v}{2(r_{h,w})} \right)^{1/2}$$

where  $(r_{h,w})$  is the hydraulic radius of the wick structure, defined as twice the area of the wick pore at the wick–vapor interface divided by the wetted perimeter at the wick–vapor interface.

The *boiling limit* occurs when the input heat flux is so high that nucleate boiling occurs in the wicking structure and bubbles may become trapped in the wick, blocking the liquid return and resulting in evaporator dryout. This phenomenon differs from the other limitations previously discussed in that it depends on the evaporator heat flux as opposed to the axial heat flux. This expression, which is a function of the fluid properties, can be written as

$$q_{b,m} = \left( \frac{2\pi L_{\text{eff}} k_{\text{eff}} T_v}{h_{fg} \rho_v \ln(r_i/r_n)} \right) \left( \frac{2\sigma}{r_n} - \Delta P_{c,m} \right)$$

where  $k_{\text{eff}}$  is the effective thermal conductivity of the liquid–wick combination, given in Table 43.27,  $r_i$  is the inner radius of the heat pipe wall, and  $r_n$  is the nucleation site radius.

After the power level associated with each of the four limitations is established, determination of the maximum heat transport capacity is only a matter of selecting the lowest limitation for any given operating temperature.

**Heat Pipe Thermal Resistance**

The *heat pipe thermal resistance* can be found using an analogous electrothermal network. Figure 43.32 illustrates the electrothermal analog for the heat pipe illustrated in Fig. 43.31. As shown, the overall thermal resistance is comprised of nine different resistances arranged in a series/parallel combination, which can be summarized as follows:

- $R_{pe}$ —the radial resistance of the pipe wall at the evaporator
- $R_{we}$ —the resistance of the liquid–wick combination at the evaporator
- $R_{ie}$ —the resistance of the liquid–vapor interface at the evaporator
- $R_{va}$ —the resistance of the adiabatic vapor section
- $R_{pa}$ —the axial resistance of the pipe wall
- $R_{wa}$ —the axial resistance of the liquid–wick combination
- $R_{ic}$ —the resistance of the liquid–vapor interface at the condenser
- $R_{wc}$ —the resistance of the liquid–wick combination at the condenser
- $R_{pc}$ —the radial resistance of the pipe wall at the condenser

**Table 43.27 Wick Permeability for Several Wick Structures**

Structure	K	Data
Circular cylinder (artery or tunnel wick)	$r^2/8$	$r$ = radius of liquid flow passage
Open rectangular grooves	$2\varepsilon(r_{h,1})^2/(f_1 Re_1) = \omega/s$	$\varepsilon$ = wick porosity $\omega$ = groove width $s$ = groove pitch $\delta$ = groove depth $(r_{h,1}) = 2\omega\delta/(\omega + 2\delta)$
Circular annular wick	$2(r_{h,1})^2/(f_1 Re_1)$	$(r_{h,1}) = r_1 - r_2$
Wrapped screen wick	$1/122 d_w^2 \varepsilon^3/(1 - \varepsilon)^2$	$d_w$ = wire diameter $\varepsilon = 1 - (1.05 \pi N d_w/4)$ $N$ = mesh number
Packed sphere	$1/37.5 r_s^2 \varepsilon^3/(1 - \varepsilon)^2$	$r_s$ = sphere radius $\varepsilon$ = porosity (dependent on packing mode)

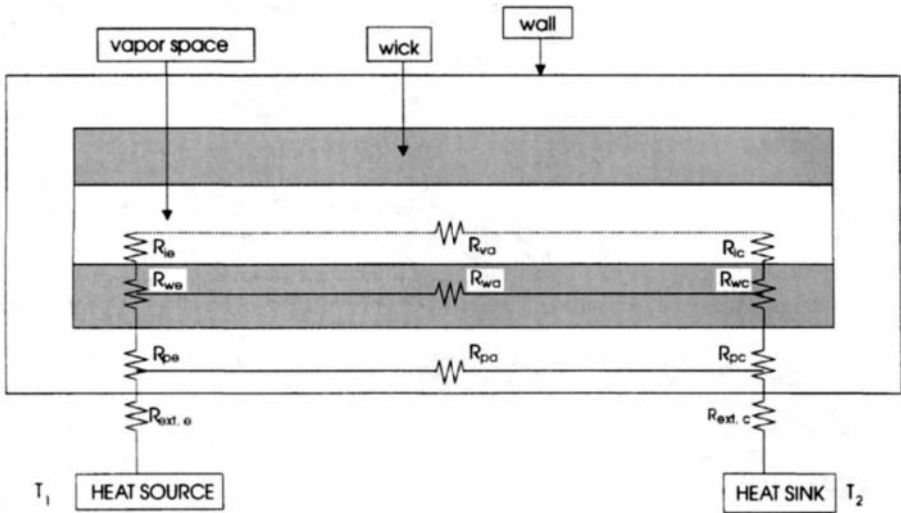


Fig. 43.32 Equivalent thermal resistance of a heat pipe.

Because of the comparative magnitudes of the resistance of the vapor space and the axial resistances of the pipe wall and liquid-wick combinations, the axial resistance of both the pipe wall and the liquid-wick combination may be treated as open circuits and neglected. Also, because of the comparative resistances, the liquid-vapor interface resistances and the axial vapor resistance can, in most situations, be assumed to be negligible. This leaves only the pipe wall radial resistances and the liquid-wick resistances at both the evaporator and condenser. The radial resistances at the pipe wall can be computed from Fourier's law as

$$R_{pe} = \frac{\delta}{k_p A_e}$$

for flat plates, where  $\delta$  is the plate thickness and  $A_e$  is the evaporator area, or

$$R_{pe} = \frac{\ln(D_o/D_i)}{2\pi L_e k_p}$$

for cylindrical pipes, where  $L_e$  is the evaporator length. An expression for the equivalent thermal resistance of the liquid-wick combination in circular pipes is

$$R_{we} = \frac{\ln(D_o/D_i)}{2\pi L_e k_{\text{eff}}}$$

where values for the effective conductivity  $k_{\text{eff}}$  can be found in Table 43.27. The adiabatic vapor resistance, although usually negligible, can be found as

$$R_{va} = \frac{T_v(P_{v,e} - P_{v,c})}{\rho_v h_{fg} q}$$

where  $P_{v,e}$  and  $P_{v,c}$  are the vapor pressures at the evaporator and condenser. Combining these individual resistances provides a mechanism by which the overall thermal resistance can be computed and hence the temperature drop associated with various axial heat fluxes can be determined.

**Table 43.28 Effective Thermal Conductivity for Liquid-Saturated Wick Structures**

Wick Structures	$k_{\text{eff}}$
Wick and liquid in series	$\frac{k_l k_w}{\varepsilon k_w + k_l(1 - \varepsilon)}$
Wick and liquid in parallel	$\varepsilon k_l + k_w(1 - \varepsilon)$
Wrapped screen	$\frac{k_l[(k_l + k_w) - (1 - \varepsilon)(k_l - k_w)]}{(k_l + k_w) + (1 - \varepsilon)(k_l - k_w)}$
Packed spheres <sup>34</sup>	$\frac{k_l[(2k_l + k_w) - 2(1 - \varepsilon)(k_l - k_w)]}{(2k_l + k_w) + (1 - \varepsilon)(k_l - k_w)}$
Rectangular grooves	$\frac{w_f k_l k_w \delta + w k_l(0.185 w_f k_w + \delta k_l)}{(w + w_f)(0.185 w_f k_f + \delta k_l)}$

**REFERENCES**

1. F. P. Incropera and D. P. Dewitt, *Fundamentals of Heat Transfer*, Wiley, New York, 1981.
2. E. R. G. Eckert and R. M. Drake, Jr., *Analysis of Heat and Mass Transfer*, McGraw-Hill, NY, 1972.
3. M. P. Heisler, "Temperature Charts for Induction and Constant Temperature Heating," *Trans. ASME* **69**, 227 (1947).
4. H. Grober and S. Erk, *Fundamentals of Heat Transfer*, McGraw-Hill, New York, 1961.
5. E. N. Sieder and C. E. Tate, "Heat Transfer and Pressure Drop of Liquids in Tubes," *Ind. Eng. Chem.* **28**, 1429 (1936).
6. F. W. Dittus and L. M. K. Baelter, *Univ. Calif., Berkeley, Pub. Eng.* **2**, 443 (1930).
7. A. J. Chapman, *Heat Transfer*, Macmillan, New York, 1974.
8. S. Whitaker, *AICHE J.* **18**, 361 (1972).
9. M. Jakob, *Heat Transfer*, Vol. 1, Wiley, New York, 1949.
10. A. Zhukauska, "Heat Transfer from Tubes in Cross Flow," in *Advances in Heat Transfer*, Vol. 8, J. P. Hartnett and T. F. Irvine, Jr. (eds.), Academic, New York, 1972.
11. F. Kreith, *Principles of Heat Transfer*, Harper and Row, New York, 1973.
12. H. A. Johnson and M. W. Rubesin, "Aerodynamic Heating and Convective Heat Transfer," *Trans. ASME*, **71**, 447 (1949).
13. C. C. Lin (ed.), *Turbulent Flows and Heat Transfer, High Speed Aerodynamics and Jet Propulsion*, Vol. 5, Princeton University Press, Princeton, NJ, 1959.
14. W. H. McAdams (ed.), *Heat Transmission*, 3rd ed., McGraw-Hill, New York, 1954.
15. T. Yuge, "Experiments on Heat Transfer from Spheres Including Combined Natural and Forced Convection," *J. Heat Transfer* **82**, 214 (1960).
16. S. Globe and D. Dropkin, "Natural Convection Heat Transfer in Liquids Confined between Two Horizontal Plates," *J. Heat Transfer* **81C**, 24 (1959).
17. I. Catton, "Natural Convection in Enclosures," in *Proc. 6th International Heat Transfer Conference*, 6, Toronto, Canada, 1978.
18. R. K. MacGregor and A. P. Emery, "Free Convection through Vertical Plane Layers: Moderate and High Prandtl Number Fluids," *J. Heat Transfer* **91**, 391(1969).
19. R. Siegel and J. R. Howell, *Thermal Radiation Heat Transfer*, McGraw-Hill, New York, 1981.
20. G. G. Gubareff, J. E. Janssen, and R. H. Torborg, *Thermal Radiation Properties Survey*, 2nd ed., Minneapolis Honeywell Regulator Co., Minneapolis, MN, 1960.
21. H. C. Hottel, in *Heat Transmission*, W. C. McAdams (ed.), McGraw-Hill, New York, 1954, Chap. 2.
22. W. M. Rohsenow, "Film Condensation," in *Handbook of Heat Transfer*, W. M. Rohsenow and J. P. Hartnett (eds.), McGraw-Hill, New York, 1973.
23. J. C. Chato, "Laminar Condensation Inside Horizontal and Inclined Tubes," *J. Am. Soc. Heating Refrig. Aircond. Engrs.* **4**, 52 (1962).

24. W. W. Akers, H. A. Deans, and O. K. Crosser, "Condensing Heat Transfer Within Horizontal Tubes," *Chem. Eng. Prog., Sym. Ser.* **55** (29), 171 (1958).
25. W. M. Rohsenow, "A Method of Correlating Heat Transfer Data for Surface Boiling Liquids," *Trans. ASME* **74**, 969 (1952).
26. J. P. Holman, *Heat Transfer*, McGraw-Hill, New York, 1981.
27. N. Zuber, "On the Stability of Boiling Heat Transfer," *Trans. ASME* **80**, 711 (1958).
28. L. A. Bromley, "Heat Transfer in Stable Film Boiling," *Chem. Eng. Prog.* **46**, 221 (1950).
29. M. Jacob and G. A. Hawkins, *Elements of Heat Transfer*, Wiley, New York, 1957.
30. G. P. Peterson, *An Introduction to Heat Pipes: Modeling, Testing and Applications*, Wiley, New York, 1994.
31. G. P. Peterson, A. B. Duncan and M. H. Weichold, "Experimental Investigation of Micro Heat Pipes Fabricated in Silicon Wafers," *ASME J. Heat Transfer* **115**, 751 (1993).
32. G. P. Peterson, "Capillary Priming Characteristics of a High Capacity Dual Passage Heat Pipe," *Chemical Engineering Communications* **27**(1), 119 (1984).
33. G. P. Peterson and L. S. Fletcher, "Effective Thermal Conductivity of Sintered Heat Pipe Wicks," *AIAA J. of Thermophysics and Heat Transfer* **1**, 36 (1987).

## BIBLIOGRAPHY

- American Society of Heating, Refrigerating and Air Conditioning Engineering, *ASHRAE Handbook of Fundamentals*, 1972.
- Arpaci, V. S., *Conduction Heat Transfer*, Addison-Wesley, Reading, MA, 1966.
- Carslaw, H. S., and J. C. Jager, *Conduction of Heat in Solid*, Oxford University Press, Oxford, 1959.
- Chi, S. W., *Heat Pipe Theory and Practice*, McGraw-Hill, New York, 1976.
- Duffie, J. A., and W. A. Beckman, *Solar Engineering of Thermal Process*, Wiley, New York, 1980.
- Dunn, P. D., and D. A. Reay, *Heat Pipes*, 3rd ed., Pergamon Press, New York, 1983.
- Gebhart, B., *Heat Transfer*, McGraw-Hill, New York, 1971.
- Hottel, H. C., and A. F. Saroffin, *Radiative Transfer*, McGraw-Hill, New York, 1967.
- Kays, W. M., *Convective Heat and Mass Transfer*, McGraw-Hill, New York, 1966.
- Knudsen, J. G., and D. L. Katz, *Fluid Dynamics and Heat Transfer*, McGraw-Hill, New York, 1958.
- Ozisik, M. N., *Radiative Transfer and Interaction with Conduction and Convection*, Wiley, New York, 1973.
- , *Heat Conduction*, Wiley, New York, 1980.
- Peterson, G. P., *An Introduction to Heat Pipes: Modeling, Testing and Applications*, Wiley, New York, 1994.
- Planck, M., *The Theory of Heat Radiation*, Dover, New York, 1959.
- Rohsenow, W. M., and H. Y. Choi, *Heat, Mass, and Momentum Transfer*, Prentice-Hall, Englewood Cliffs, NJ, 1961.
- Rohsenow, W. M., and J. P. Hartnett, *Handbook of Heat Transfer*, McGraw-Hill, New York, 1973.
- Schlichting, H., *Boundary-Layer Theory*, McGraw-Hill, New York, 1979.
- Schneider, P. J., *Conduction Heat Transfer*, Addison-Wesley, Reading, MA, 1955.
- Sparrow, E. M., and R. D. Cess, *Radiation Heat Transfer*, Wadsworth, Belmont, CA, 1966.
- Tien, C. L., "Fluid Mechanics of Heat Pipes," *Ann. Rev. Fluid Mechanics*, 167 (1975).
- Turner, W. C., and J. F. Malloy, *Thermal Insulation Handbook*, McGraw-Hill, New York, 1981.
- Vargafik, N. B., *Table of Thermophysical Properties of Liquids and Gases*, Hemisphere, Washington, DC, 1975.
- Wiebelt, J. A., *Engineering Radiation Heat Transfer*, Holt, Rinehart and Winston, New York, 1966.